Journal of Structural Geology 32 (2010) 423–444

Contents lists available at ScienceDirect

Journal of Structural Geology

journal homepage: www.elsevier.com/locate/jsg

Structural geometry of an exhumed UHP terrane in the eastern Sulu Orogen, China: Implications for continental collisional processes

Lu Wang [a,b], Timothy M. Kusky [a,b,*], Sanzhong Li [b]

[a] State Key Laboratory of Geological Processes and Mineral Resources and Three Gorges Geohazards Research Center, Ministry of Education, China University of Geosciences Wuhan, 388 Lumo Road, Wuhan 430074, China
[b] Department of Marine Geology, Ocean University of China, 238 Songling Road, Qingdao 266100, China

ARTICLE INFO

Article history:
Received 31 March 2009
Received in revised form
25 January 2010
Accepted 30 January 2010
Available online 17 February 2010

Keywords:
Yangkou
UHP metamorphism
Structural mapping
Sulu orogen
Superimposed folding

ABSTRACT

High-precision 1:200–1:1000 mapping of Yangkou Bay, eastern Sulu orogen, defines the structural geometry and history of one of the world's most significant UHP (ultrahigh-pressure) belts. At least four stages of folds are recognized in UHP eclogites and associated quartzo-feldspathic gneiss. UHP eclogite facies rootless F_1 and isoclinal F_2 folds are preserved locally in coesite-eclogite. Mylonitic to ultramylonitic quartzo-feldspathic and coesite-eclogite shear zones separate small-scale 5–10-m-thick nappes of ultramafic-mafic UHP rocks from banded quartzo-feldspathic gneiss. These shear zones are folded, and progressively overprinted by amphibolite-greenschist facies shear zones. The prograde to retrograde D_1–D_5 deformation sequence is explained by deep subduction of offscraped thrust slices of lower continental or oceanic crust from the down-going plate, caught between the colliding North and South China cratons in the Mesozoic. After these slices were structurally isolated along the plate interface, they were rolled in the subduction channel during exhumation and structural juxtaposition with quartzo-feldspathic gneisses, forming several generations of folds, sequentially lower-grade foliations and lineations, and intruded by in situ and exotically derived melts. Shear zones formed during different deformation generations are wider with lower grades, suggesting that deep-crustal/upper mantle deformation operates more efficiently, perhaps with more active crystallographic slip systems, than deformation at mid-upper crustal levels.

1. Introduction

Understanding deep crustal deformational and metamorphic processes associated with continental collision has advanced greatly in recent years with numerous studies of exhumed HP and UHP metamorphic rocks from classical localities around the world, including the Dora Maria area of the western Alps, the Western Gneiss region of the Caledonian belt in Norway, and in the 1500 km long Qinling-Dabie Sulu orogen of eastern China (e.g. Baldwin et al., 2005; Brown and Piccoli, 2006; Brown and Rushmer, 2006; Brueckner and van Roermund, 2004; Chemenda et al., 1997; Chopin, 1984, 2003; Hacker et al., 2006, 2009; Liu et al., 2006; Maruyama et al., 1994; Molina et al., 2002; Okay and Sengor, 1992; Okay et al., 1993; Smith, 1984; Sobolev and Shatsky, 1990; Stefan et al., 2004; Wiesinger et al., 2006; Zheng et al., 2003). Analysis of metamorphic *P–T* conditions and processes has advanced at a faster pace than studies of the deformation mechanisms at UHP conditions, and of the detailed structure of the belts that contain the UHP rocks (e.g., Wallis et al., 1997, 1999, 2005; Xue et al., 1996). In this contribution we present a detailed structural analysis of an exceptionally well-exposed UHP terrain that contains some of the highest-pressure UHP rocks known on Earth, Yangkou Bay on the Shandong Peninsula of China's Sulu belt.

Previous studies (Wallis et al., 1997, 1999; Lin et al., 2009; Faure et al., 2003; Ratschbacher and Hacker, 2000; Ratschbacher et al., 2006; Suo et al., 2000) on the multi-stage deformation in the Dabie-Sulu belt show that the main preserved deformation structures formed under amphibolite facies conditions. Ideas for why blocks containing UHP eclogite facies deformation fabrics are rare have been diverse, including: (1) few of the structural lenses may have been brought to depths great enough to experience UHP conditions; (2) the long exhumation path was associated with retrogression; (3) strong overprinting by younger deformation and metamorphism; and (4) localized development of the initial

* Corresponding author. State Key Laboratory of Geological Processes and Mineral Resources and Three Gorges Geohazards Research Center, Ministry of Education, China University of Geosciences Wuhan, 388 Lumo Road, Wuhan 430074, China. Fax: +86 27 67885096, 189 7157 9211.
E-mail address: tkusky@gmail.com (T.M. Kusky).

0191-8141/$ – see front matter © 2010 Elsevier Ltd. All rights reserved.
doi:10.1016/j.jsg.2010.01.012

structures was restricted to narrow shear zones. Zhao et al. (2003) reported several localities of UHP shear zones in Sulu belt including Yangkou, the focus of this study.

The reason Yangkou Bay is so important for geologists is because (1) it preserves one of most rare and significant occurrences of garnet peridotite and coesite-bearing UHP (ultrahigh-pressure) ecolgite containing interstitial coesite, (2) it shows evidence for UHP conditions affecting granitic rocks, and (3) it preserves pre-eclogite facies deformation fabrics (Hirajima, 1996; Hirajima et al., 1993; Jahn, 1998; Liou and Zhang, 1996; Yoshida et al., 2004; Wallis et al., 2005). Petrologic study reveals rare intergranular coesite (Liou and Zhang, 1996; Ye et al., 1996; Wallis et al., 1997) and high concentrations of clinopyroxene, rutile and apatite exsolution lamellae in garnet within eclogite, which may indicate very deep continental subduction exceeding 200 km in a dry environment, followed by fast exhumation (Ye et al., 2000a,b). However, the interpretation of depths exceeding 200 km has recently been challenged by Hwang et al. (2007). Yangkou is also exceptional in that it is rare to find preserved locations in the Dabie-Sulu belt where different metamorphic stages and deformation events spanning the whole subduction and exhumation process can be documented, including details about the internal structure, over-printing relationships between different generations of structures and metamorphic fabrics, and relationships to bounding units. All of these relationships are exposed clearly in nearly continuous coastal exposures within a range of 1 km^2 at Yangkou, making this a classical location to test relationships between deformational and metamorphic processes associated with subduction and exhumation of continental rocks from 200 km to the surface. Despite Yangkou having proven to be a testing ground of metamorphic theories, few studies of the complex structural relationships in this region have been undertaken and the geologic history is not yet completely understood (Wallis et al., 1997; Fang and Zhao, 2004; Zhao et al., 2003, 2005).

Results of new detailed and targeted high-precision 1:200–1:1000 field mapping on the nearly continuous coastal exposures are presented here as a basis for understanding the structural sequence of the lenses that contain the UHP assemblages at Yangkou, and their relationship to surrounding HP and lower-grade rocks. Comprehensive field, structural and petrofabric studies of the UHP and other rocks in the Yangkou exposures reveal a sequence of four folding events at different metamorphic grades, associated with parts of the prograde and the retrograde path of the UHP rocks formed as they completed their circuit from the surface to >200 km depth, and back to the surface, separated by partial melting and igneous intrusion events. Preliminary data indicates that UHP metamorphism was associated with formation of a series of ~5–10s of meters wide fold nappes bounded by cm-decameter thick shear zones, and that deformation at progressively lower grades of metamorphism was associated with formation of progressively wider shear zones as the metamorphism entered the realm of regional amphibolite and greenschist facies conditions.

2. Regional geology

The Sulu belt of China's Shandong Peninsula represents the eastern extension of the Qinling-Dabie orogenic belt (Meng and Zhang, 2000; Oh and Kusky, 2007; Hacker et al., 2009; Li et al., 2009), formed by subduction of oceanic lithosphere leading to the collision of the Yangtze and North China cratons and deep subduction of intervening continental material (inset of Fig. 1), possibly including an eastern extension of the Qinling micro-continent from the Dabie orogen (Hacker et al., 2009). There have been many studies in the Sulu belt on the UHP metamorphism, petrology, geochronology, geochemistry, geophysics, and structural

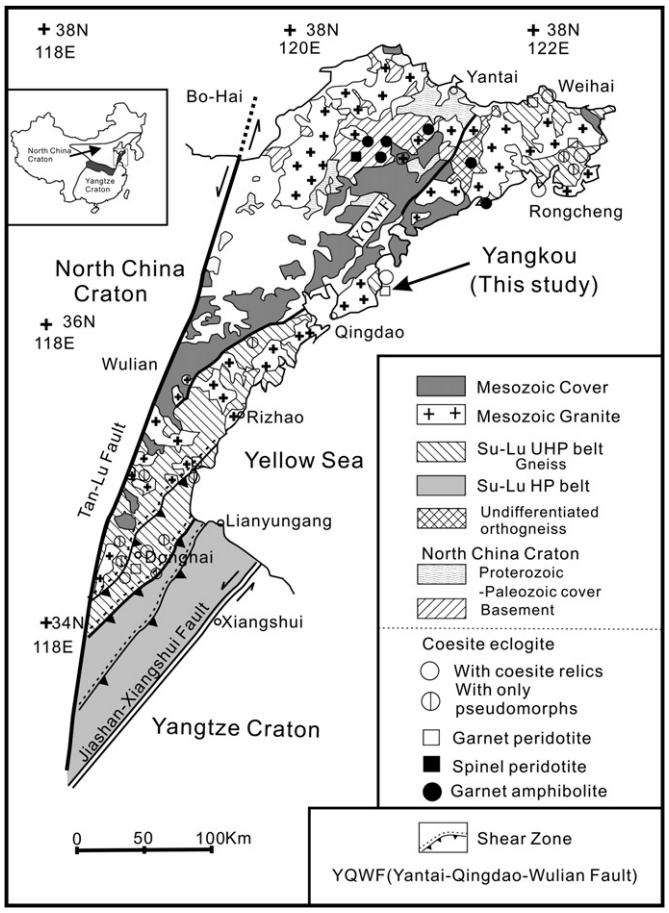

Fig. 1. Geological map of the Su-Lu ultrahigh-pressure (UHP) metamorphic belt (after Yoshida et al., 2004). Inset shows location of the Sulu Belt at the eastern end of the Qinling-Dabie orogen.

environment of UHP metamorphism and exhumation (Ames et al., 1996; Hacker et al., 1995, 1998, 2004, 2006; Li et al., 2001; Liu et al., 1994; Wallis et al., 1997, 1999; Ye et al., 2000b). However, structural analysis has lagged behind the metamorphic studies and has been largely restricted to investigation of the deep-level continental subduction processes at the thin section to lattice scales (e.g., Jin et al., 2001; Zhang et al., 1996, 2006; Wang et al., 2010). The timing of the collision, nature of pre-collision subduction systems, intervening crustal blocks, geometries of subduction, and causes of the deep continental subduction and later exhumation have all been controversial topics (e.g., Cheng et al., 2000; Hacker et al., 1998, 2006, 2009; Ratschbacher et al., 2000, 2006; Katsube et al., 2008; Li et al., 2007, 2009; Liu et al., 2005; Zheng et al., 2004). A basic framework for the evolution of the Sulu Belt includes rifting of Rodinia about 800 Ma ago, leading to the formation of an ocean basin. This basin developed arc systems by the early Paleozoic, including a fragment of the Yangtze craton (Qinling micro-continent), that collided with the NCC. Later, in the Mesozoic, subduction brought the leading edge of Yangtze beneath the Dabie-Sulu orogen and the North China craton and intervening Qinling microcontinent in some parts of the orogen, leading to continental subduction and the formation of UHP assemblages.

The Sulu belt is exposed on the southern half of the Shandong Peninsula, with Archean and Paleoproterozoic gneisses of the North China craton (Kusky and Santosh, 2009) occupying the northern part of the peninsula (Fig. 1). Several Mesozoic (mostly Cretaceous) basins associated with the Tanlu strike-slip fault system occupy the central part of the peninsula, structurally overlying rocks of the

Sulu belt and the North China craton. The main faults of this set are generally parallel to the sinistral Tanlu fault that defines the western side of the peninsula, showing that the region was affected by significant Cretaceous and younger deformations. The Yantai-Qingdao-Wulian fault is generally taken as the boundary between the Sulu belt to the south, and the North China craton to the north, but other recent studies (e.g., Faure et al., 2003; Hacker et al., 2006, 2009) suggest that this fault marks the boundary between the Sulu belt (subducted Yangtze craton) and the Qinling microcontinent to the north, and the North China craton boundary is located further to the north. This fault exhibits top down to the NW and sinistral components of movement, and has yielded $^{40}Ar/^{39}Ar$ (muscovite) ages of 146 Ma (Yang et al., 1997). Cretaceous granites with U–Pb ages falling between 120 and 110 Ma (Guo et al., 2002; Zhao et al., 1998) intrude all three of the main lithotectonic units, and include the Mt. Laoshan complex on the western side of the Yangkou Bay exposure (circa 130–120 Ma) hornblende and biotite $^{40}Ar/^{39}Ar$ closure temperatures, with K-feldspar $^{40}Ar/^{39}Ar$ cooling ages extending to 100 Ma (Liu et al., 2005; Hacker et al., 2009).

The Laoshan intrusive complex has numerous phases (Fig. 2), including fine-medium-coarse grained alkaline granite, porphyritic medium-fine grained alkaline granite, fine-medium grained orthoclase granite and medium grained monzogranite, including quartz porphyry dikes that cut the outcrops at Yangkou Bay, serving as a late time marker for different stages of deformation.

The Sulu belt extends for ~500 km across the Shandong Peninsula, and consists of quartzo-feldspathic gneiss with numerous tectonically bounded coesite-bearing eclogite lenses, ultramafic rocks including garnet peridotite, and marble. Most of the belt preserves greenschist to amphibolite facies mineral assemblages, but detailed petrological studies (e.g., Ye et al., 2000a, b; Liou et al., 2001; Wallis et al., 1997, 1999) have documented coesite inclusions in zircon grains, indicating an early UHP facies event in the Late Triassic (Ames et al., 1993; Liou and Zhang, 1996). Recent work by Hacker et al. (2006, 2009) suggest an earlier UHP event may also have occurred in the region, consistent with our observations of a UHP event followed by a HP event in the Yangkou UHP unit. The southern part of the Sulu belt is marked by a belt of blueschist-facies rocks, the northern border of which is located near Lianyungang in the northern part of Jiangsu Province (Qiu et al., 2003). The contact between the Sulu belt and the blueschist is obscured by cover, but seismic surveys suggest that this is a south-dipping normal fault (Yang, 2002; Zhao et al., 2003).

3. Yangkou Bay geology

Outcrops of the Yangkou UHP eclogite are located on the east side of the Mesozoic Laoshan intrusive complex, about 60 km east of Qingdao (Fig. 2). Detailed 1:1000 mapping of the nearly continuous exposures indicates that the outcrops at Yangkou Bay are dominated by strongly foliated UHP felsic gneiss with boudins and structural windows of ultramafic rocks, fine- and coarse grained eclogite with gabbroic textures, and amphibolites formed from retrogressed eclogite. Mylonitic to ultramylonitic shear zones separate small-scale 5–10-m-thick nappes of ultramafic-mafic UHP rocks and banded felsic gneiss, also with ultramafic lenses (Fig. 3). We divide the different rock types into two separate rock series, including an ultramafic-mafic igneous series, and a quartzo-

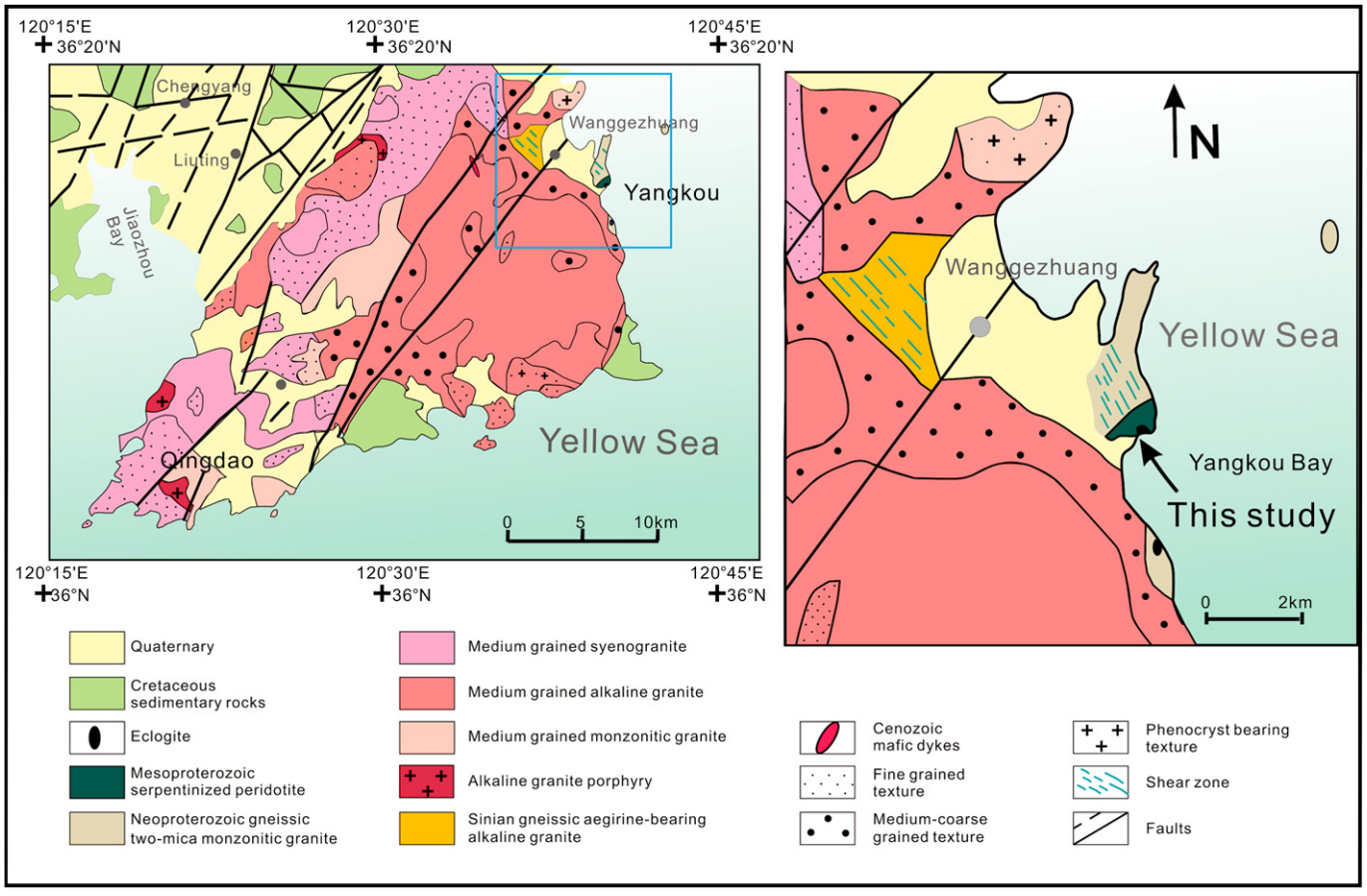

Fig. 2. Geological Map of Mt. Laoshan and the structural setting of Yangkou Bay (after Song et al., 1984).

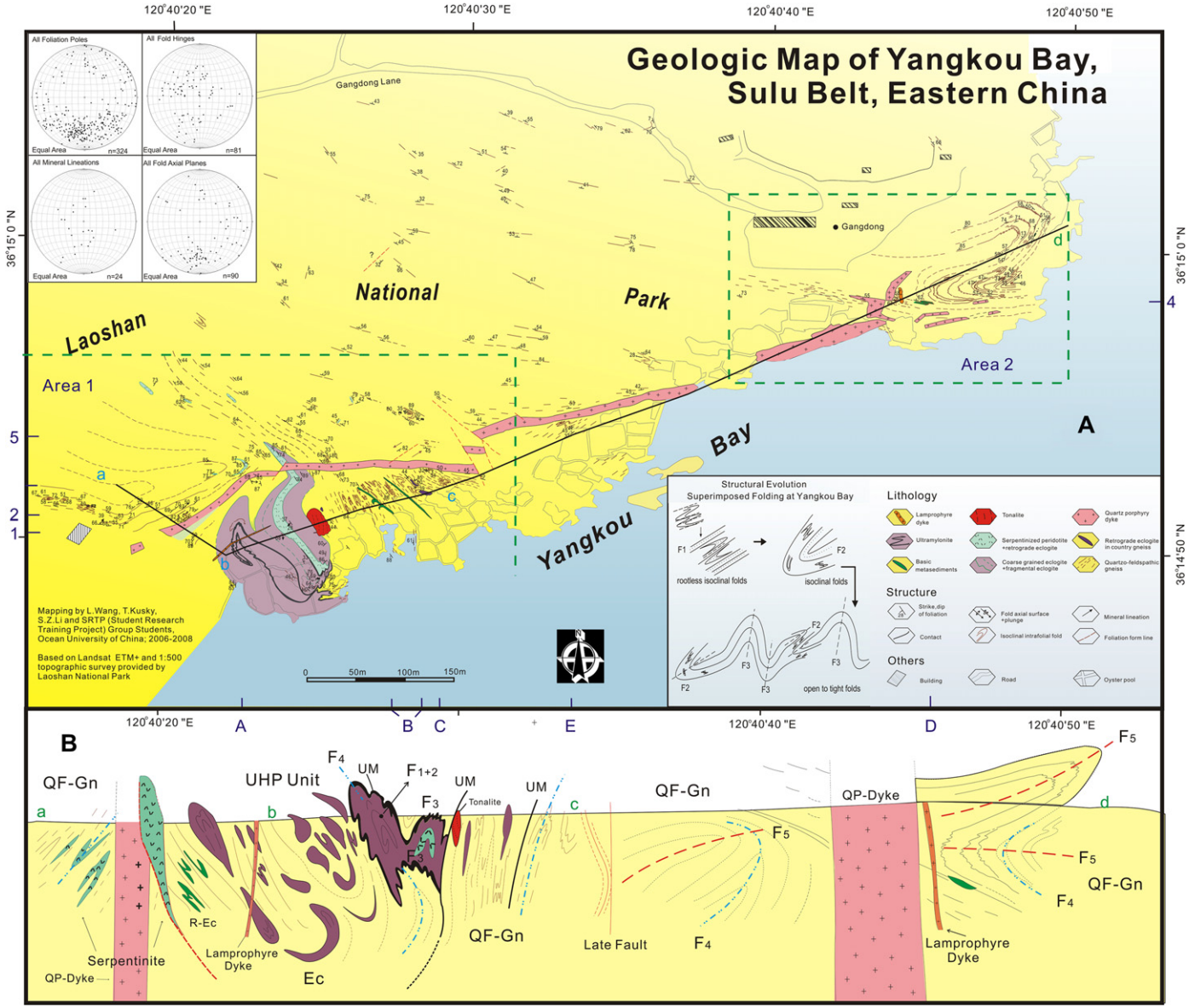

Fig. 3. (A) Detailed structural and lithological map of Yangkou. A- horizontal coordinate, 1-vertical coordinate, A-1 (and similar letter-number pairs) correspond to locations discussion in the text. Boxes indicating detailed map areas correspond to Figs. 6 (Area 1) and 7 (Area 2). (B) Interpretative cross-section drawn along profile A–B–C, in part modified after Wallis et al. (1997).

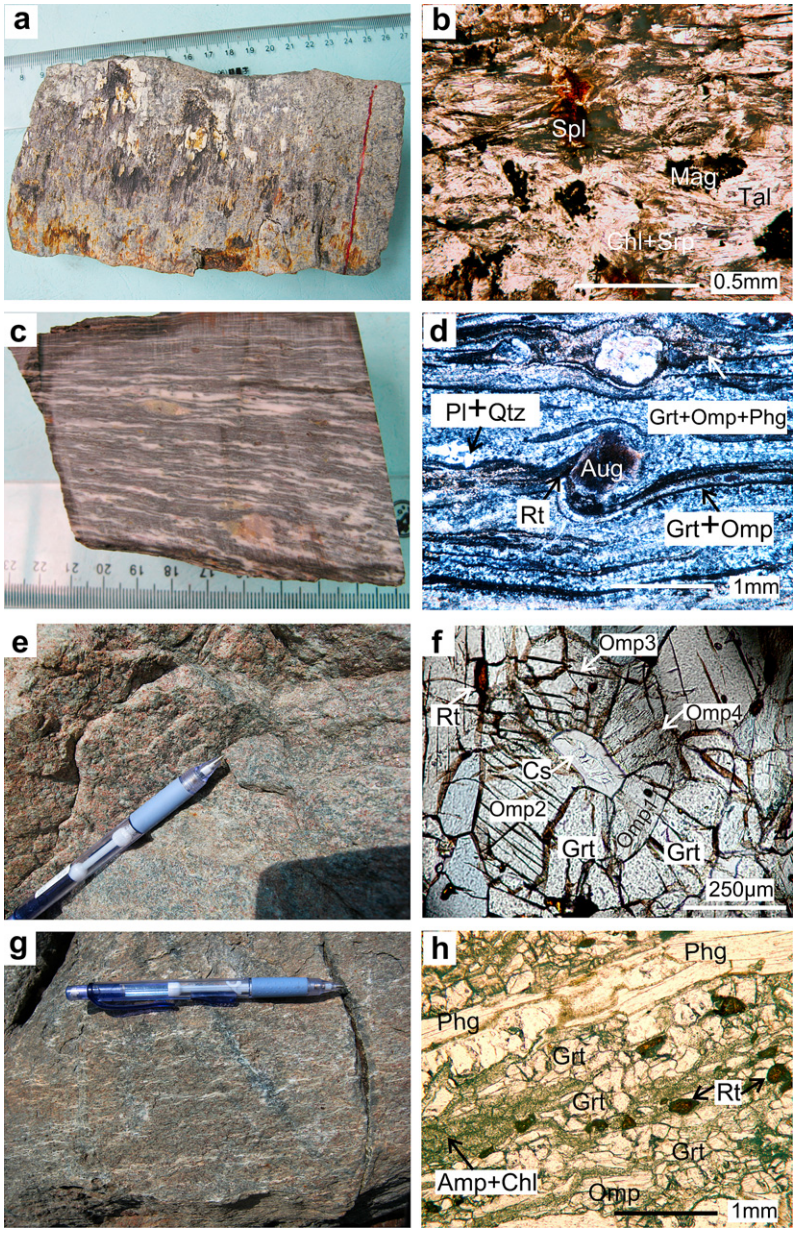

Fig. 4. Field photographs and thin section photomicrographs of the mafic-ultramafic magmatic series, varying from serpentinized talc-peridotite and gabbroic eclogite to eclogite. (a) serpentinized peridotite, (b) photomicrograph of serpentinized peridotite, mineral assemblage is chlorite + talc + serpentine + spinel + mgt; (c, d) gabbroic eclogite and its photomicrograph, mineral assemblage is plagioclase + quartz + garnet + omphacite + rutile + phengite; (e, f) garnet-rich massive eclogite and its photomicrograph, the mineral assemblage is garnet + omphacite + phengite; (g, h) retrogressed foliated eclogite and its photomicrograph. Smaller grains of garnet have grown around retrogressed omphacite (amphibole + albite).

feldspathic to metaluminous series, which we interpret to have formed separately and were later brought together during the folding and shearing events described in this contribution.

There is a wide range of ages reported from the Yangkou UHP gneiss, eclogite, and other units, but many of these ages were reported from samples taken before detailed structural mapping was completed, and it is difficult to correlate regional ages with the many different outcrop scale map units reported here, and detailed geochronology is in progress. Past age determinations are summarized by Hacker et al. (2009), who concluded that what is needed is precise outcrop scale mapping followed by detailed geochronology to understand the complexities preserved in the Sulu belt. Hacker et al. (2009) summarize U–Pb zircon ages for Precambrian orogenesis from the Yangkou area at 1.9 Ga, 852 and 796 Ma (Hu et al., 2004), 728, 793, and 795 and 625 Ma (Hacker et al., 2006), 755, 760 and 783 Ma (Leech et al., 2006), 736, 752, 757, 758 and 719 ± 4 Ma (Wu et al., 2004), 731 and 762 Ma (Ames et al., 1996). They also report zircon ages for metamorphism and local partial melting of 216 + 3/−2.4 Ma (Hacker et al., 2006), $^{40}Ar/^{39}Ar$ ages on feldspar of 196–110 Ma, $^{40}Ar/^{39}Ar$ ages on white mica of 201–189 Ma, and 128.2+/0.7 Ma (Webb et al., 2006).

3.1. Igneous rocks and their metamorphic equivalents

3.1.1. UHP unit – Serpentinized peridotite, coarse grained eclogite and fragmental eclogite, retrogressed eclogite

In the center of detailed map area 1 (Fig. 3) a relatively weakly deformed UHP unit representing a metamorphosed mafic/ultramafic magmatic series includes serpentinized peridotite, gabbroic eclogite, basaltic eclogite, fresh eclogite and retrograded eclogite

(Fig. 4), completely surrounded by UHP shear zones composed of strongly deformed eclogite facies mylonites and ultramylonites.

Serpentinized peridotites are grey-green to dark green, with a fine-grained texture. Coarse grained serpentine has grown along many joint planes. Fresh peridotite is rare and many outcrops have recently been destroyed by the local population during exploration and artisinal mining of the rock which is known locally as Laoshan Jade. Detailed petrologic work on fresh garnet peridotite from this outcrop was discussed by Yoshida et al. (2004) and Zhang et al. (2000), who estimated peak metamorphic conditions to range from ~730 to 760 °C and 3.6–4.1 Gpa. We suggest that the mantle fragment (garnet peridotite) and the crustal fragment (eclogite) in the Yangkou UHP unit both experienced a common UHP metamorphic event, and were then brought into structural contact with the surrounding quartzo-feldspathic gneisses along UHP eclogitic shear zones. These rocks were then exhumed as part of a larger crustal mass along with the surrounding quartzo-feldspathic gneisses (Yoshida et al., 2004), which also developed ultramylonite zones along its contacts with the eclogite and ultramafic units. Fig. 4a and b show a typical texture of retrogressed peridotite. In this sample, large aggregates of flaky chlorite crystals are well developed. Fiber-shaped talc and serpentine grains are larger than the common matix-forming phases and show wavy extinction, with random alignment of the talc in foliation planes, suggesting static growth of the talc along chemically favorable planes. Platy spinel is

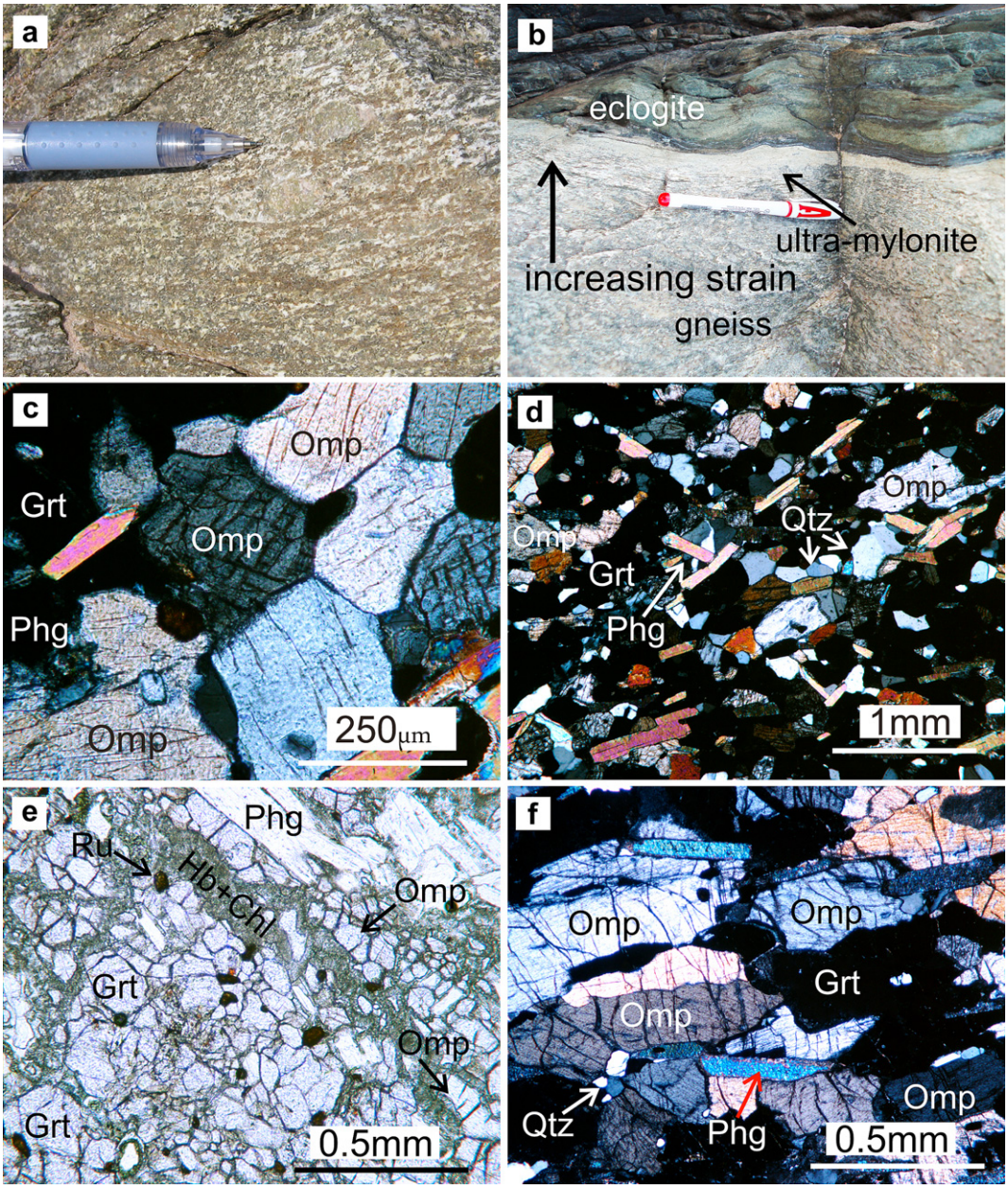

Fig. 5. (a) Outcrop photo of quartzo-feldspathic augen gneiss; (b) ultramylonite seperating eclogite mylonite and foliated quartzo-feldspathic gneiss; (c) photomicrograph of fresh foliated eclogite defined by omphacite, garnet + phengite. Foliation is first eclogite facies foliation S_1. d) photomicrograph of weakly foliated fine-grained eclogite, sample was taken from small tight F_2 fold in Fig. 9. Foliation defined by stretched garnet and omphacite, phengite shows different orientations than the early eclogite facies foliation S_1. (e) and (f) Strongly foliated retrogressed eclogite with matrix of rootless isoclinal folds, recrystallized garnet. Field of view is 2.5 mm in all photomicrographs.

irregular in shape and shows dark brown color and homogeneity. The other retrograde opaque phase is magnetite, which forms thin films surrounding the matrix spinel (Fig. 4b).

Coarse grained eclogite and fragmental eclogite, is dark green, with a coarse-medium grained faint relict gabbroic texture (Fig. 4c). It is mainly composed of omphacite + garnet + rutile + quartz and contains an igneous assemblage of Pl + Aug + Opx + Qtz + Bi + Ilm/Ti-Mag and shows relict magmatic textures and reaction coronas. Detailed petrologic study by Zhang and Liou (1997) showed that the protolith of this rock was most likely gabbro.

Foliations and lineations (S_0, S_1, L_1) are well-developed in the gabbroic eclogite, cropping out with eclogitic mylonite. Our observations show that the protoliths of these rocks range from basaltic to gabbroic to dioritic. Most minerals except augite and some quartz are sheared into bands (Fig. 4d). Quartz, augite, and quartz-feldspar aggregates are preserved as remnant porphyroclasts, in a ductile matrix of feldspar, mica, and ribbons of ductily deformed quartz. These sheared porphyroclasts are typically mantled by small grains of omphacite ± garnet, which are also present in the deformed tails of augite grains. Rutile is preferentially crystallized in pressure shadows. Plagioclase is decomposed to garnet, zoisite, kyanite and albite. The fine-grained garnet, omphacite and rutile are not only in the mantle and tail but also aggregated along the shear bands. K-feldspar and mica are dynamically recrystallized into very fine grains (see Fig. 4d). UHP–HP minerals such as omphacite, garnet and rutile in the mantles, tails, and pressure shadows of the porphyroclasts are consistent with UHP deformation (Zhao et al., 2005).

Eclogite is dark green in color and has a medium-fine grained texture. We recognize at least four metamorphic stages in the Yangkou eclogite, including one UHP eclogite facies event, one eclogite event, plus amphibolite and greenschist facies retrogressive events. This is consistent with recent dating results summarized in Hacker et al. (2006, 2009), where they document two eclogite facies events, including a precursor UHP event from 244 to 236 Ma, and a second UHP eclogite event from 230 to 220 Ma, in the Dabie-Sulu orogen, followed by an amphibolite facies event between 219 and 210 Ma.

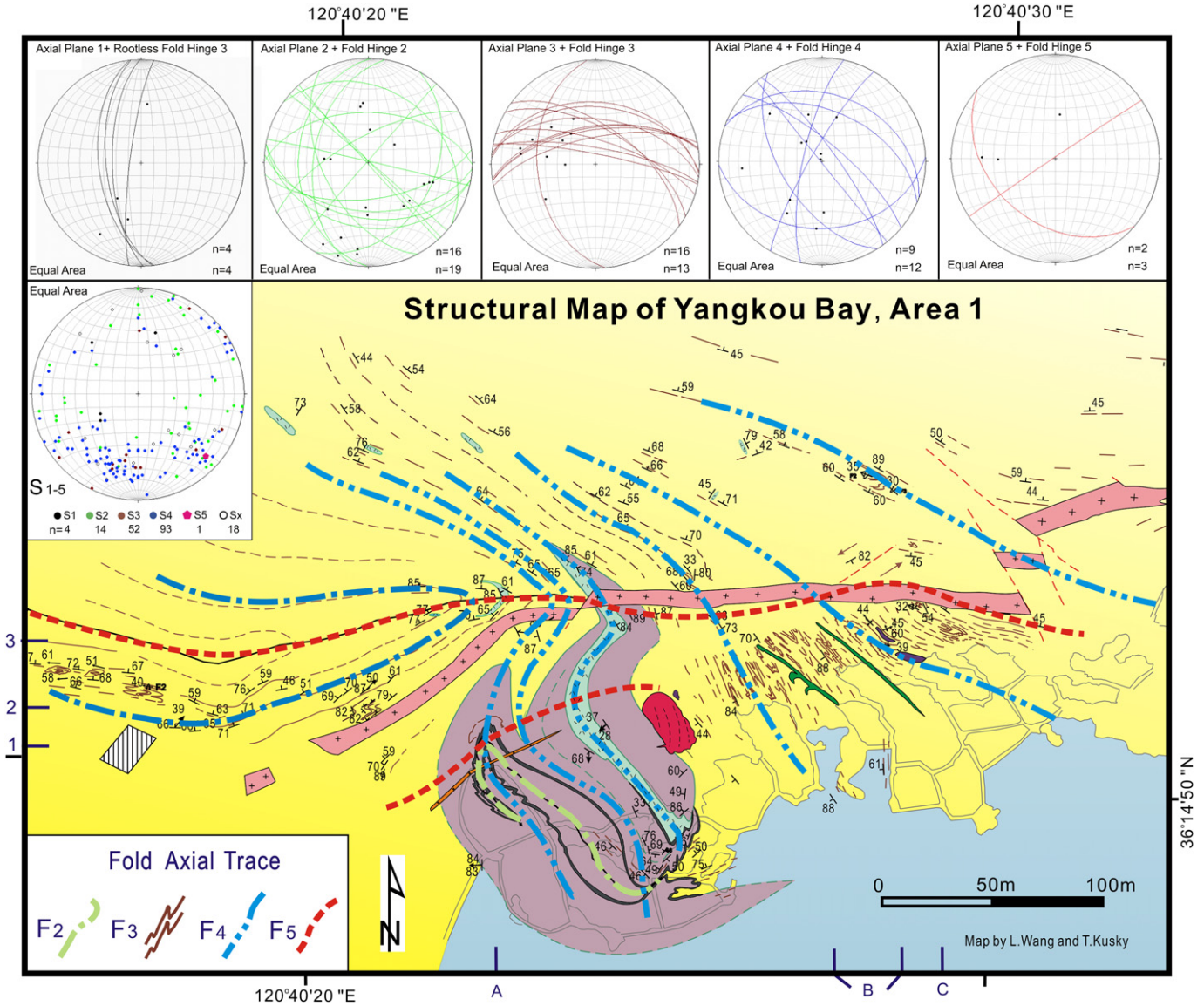

Fig. 6. Detailed structural map of Area 1 (Fig. 3), showing fold axial traces for fold generations F_2 through F_5. F_1 folds are rootless isoclinal folds, which are too small to plot on map. Lower-hermisphere equal area projections show the orientation of different foliations, fold axial planes, and fold hinges for each generation in this detailed map area.

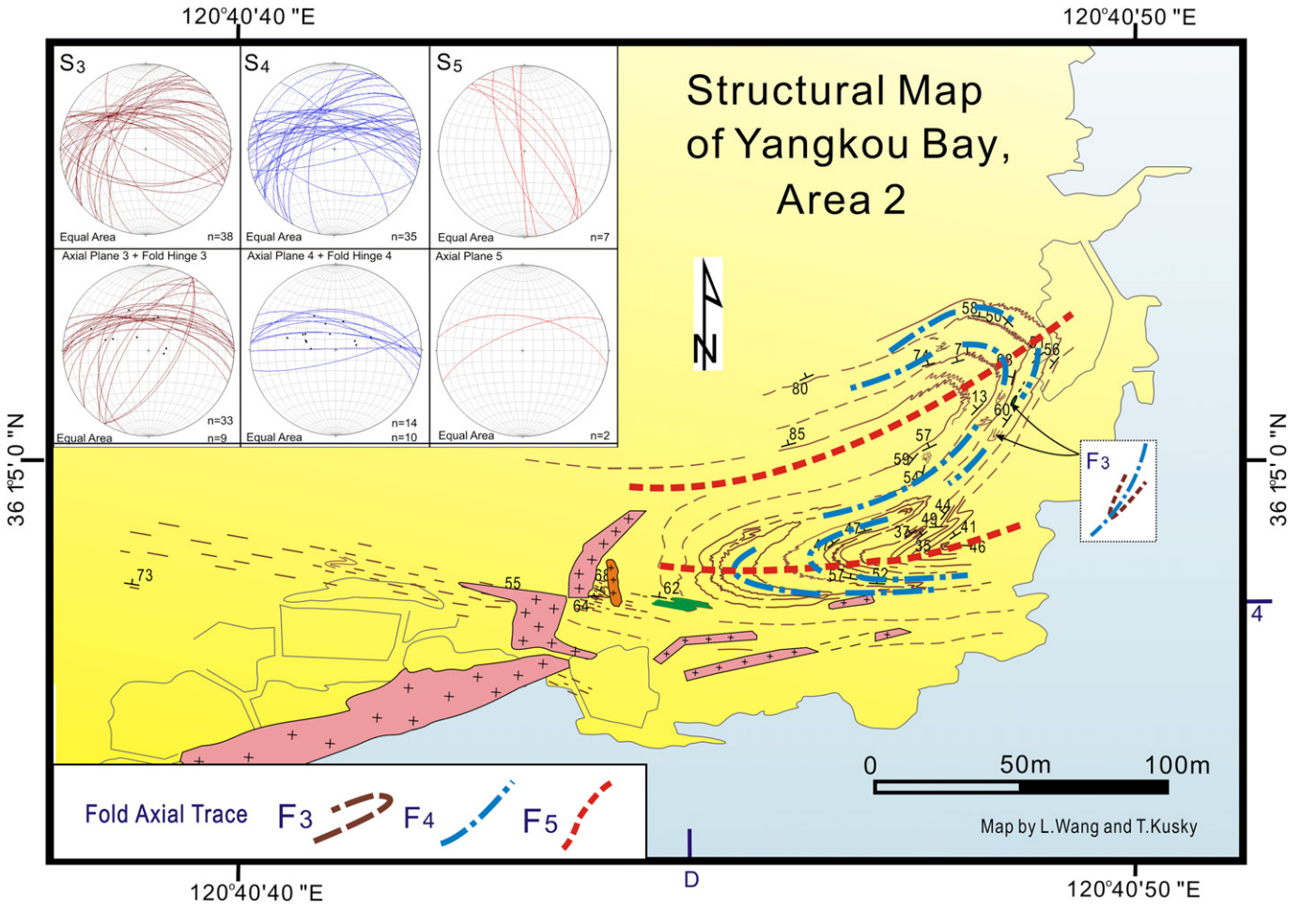

Fig. 7. Detailed structural map of Area 2 (Fig. 3), showing fold axial traces for fold generations F_3 through F_5. Lower-hemisphere equal area projections show the orientation of different foliations, fold axial planes, and fold hinges for each generation in this detailed map area.

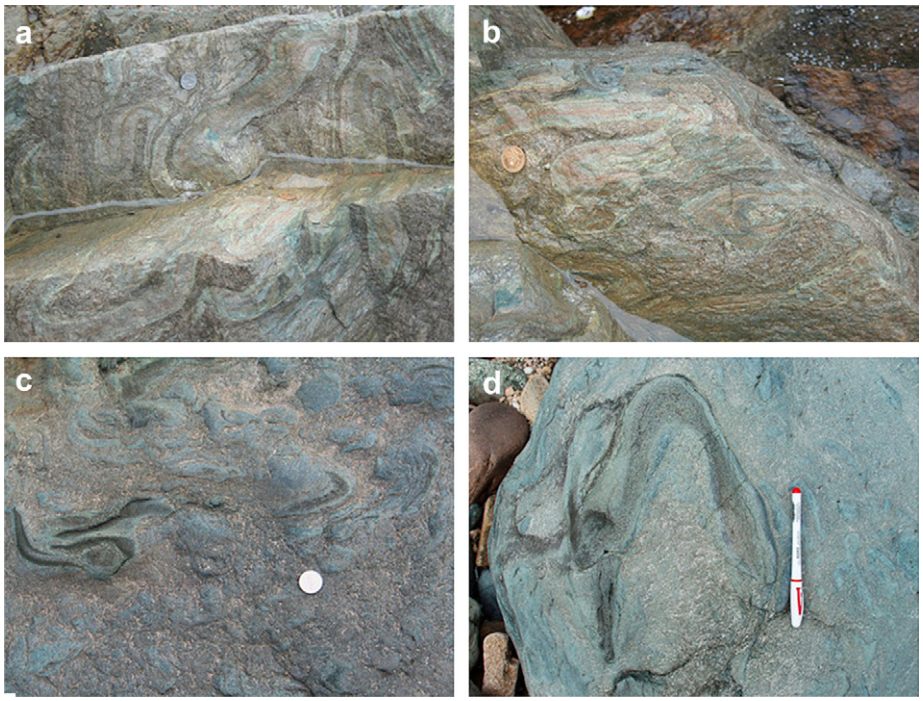

Fig. 8. (a) F_1 rootless isoclinal refolded-folds within basaltic eclogite, which gives the rock a fragmental appearance in places: (b) Fine-grained basaltic eclogite within F_1 isoclinal fold: (c) Folded layering interpreted as primary compositional layering S_1, which is different from the strongly foliated (S_2, L_2) in the matrix. The nature of the primary layering is uncertain, whether a layered igneous plutonic rock, or perhaps even a pillow-lava like fragmental volcanic. (d) Shows isolated refolded isoclinal F_1 folds in basaltic eclogite, with the fold interference pattern resembling a fragmental volcanic rock.

In zones where the eclogite is only weakly deformed (such as in F_1 fold hinges; Fig. 4e), rare coesite relics are preserved in the center of omphacite and garnet inclusions and surrounded by radiating fractures in the host minerals, representing peak UHP metamorphism. Intergranular coesite (Fig. 4f) which was described in contact with garnet and omphacite by Ye et al. (1996), Liou and Zhang (1996) and Wallis et al. (1997) is also found in weakly deformed eclogite. In relatively weakly deformed zones, statically recrystallized garnet and omphacite are aligned with a weak preferred orientation (S_1).

Most coesite inclusions have been transformed into palisade quartz and quartz pseudomorphs after coesite, representing high pressure quartz-eclogite facies metamorphism (Figs. 4f and 5c). The rock assemblage is Omp + Grt + Phg + Ru + Qtz. Rutile, polymorphed quartz, and zircon occur as inclusions in host garnet and omphacite. Rare rutile and quartz (5%) are also present in the matrix. Very thin layered coronas have grown around the rims of omphacite. Phengite grew between garnet and omphacite and typically shows straight grain boundaries. Due to different deformation behavior, eclogite in different locations exhibits different fabrics. Omphacite and garnet form a weak S_0 in weakly deformed lenses, which is slightly different than the shape orientation of later-grown phengite. Phengite and omphacite both have straight grain boundaries. In foliated eclogite, all the high pressure minerals, including omphacite, garnet, phengite and rutile, define the same S_2.

High grade amphibolite facies retrograded eclogite is represented by the mineral assemblage altered omphacite + garnet + zoisite + phengite + rutile/ilmenite. Coronas are well developed around omphacite and phengite. Omphacite and quartz reacted in these coronas to produce riebeckite and plagioclase. Isolated zoisite porphyroblasts show typical ink-blue interference colors. The assemblage phengite + zoisite + quartz (Fig. 4g) represents high pressure metamorphic conditions. The quartz fingers texture (Fig. 4g) is interpreted as an intermediate-stage decompression fabric, since it preserves retrogressed amphiboles between quartz grains.

Retrogressed amphibolite represents the low amphibolite-greenshist facies metamorphism with the mineral association (S_3)

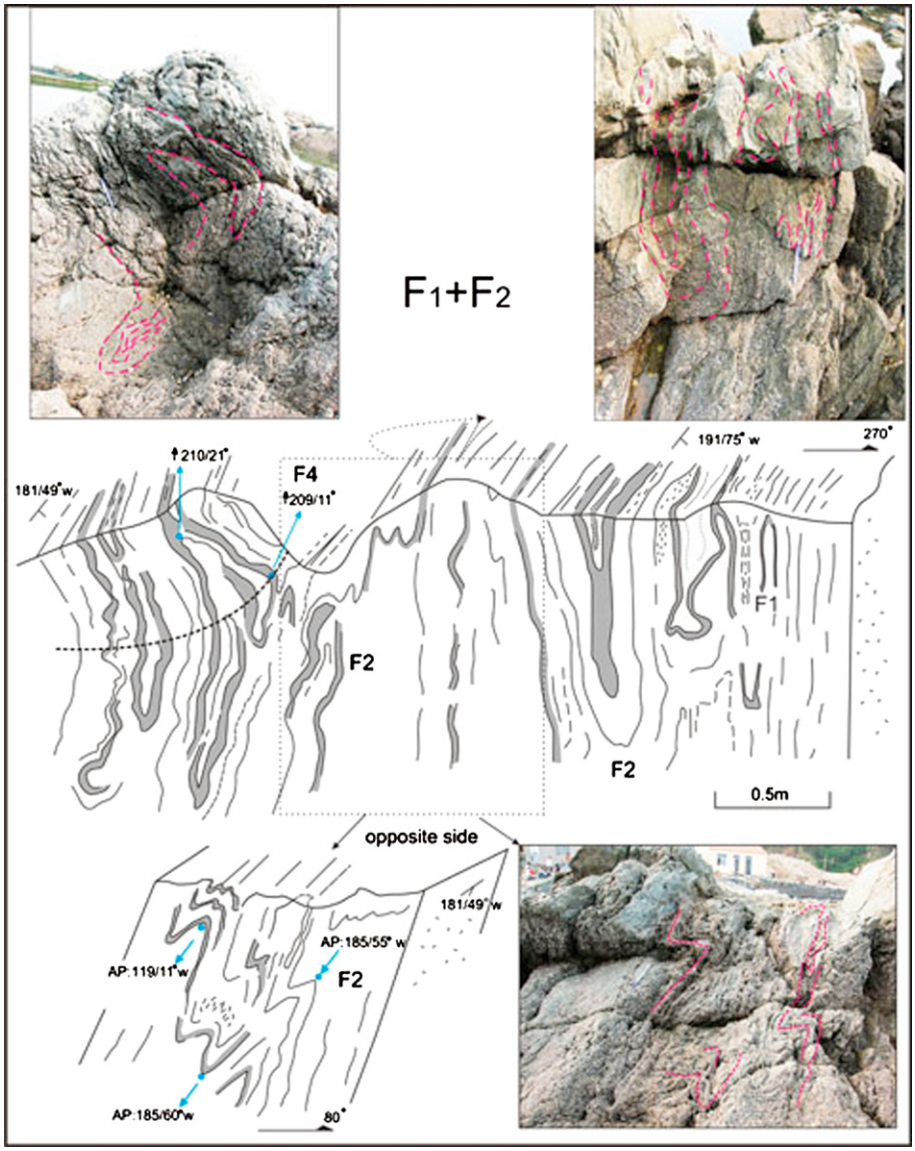

Fig. 9. F_2 eclogite facies isoclinal folds in UHP eclogite; note most of the fold axial surfaces dip steeply, and that rootless isoclinal F_1 folds can be found within the F_2 folds. Fig. 8 shows field photographs of some of the F_1 folds from this outcrop.

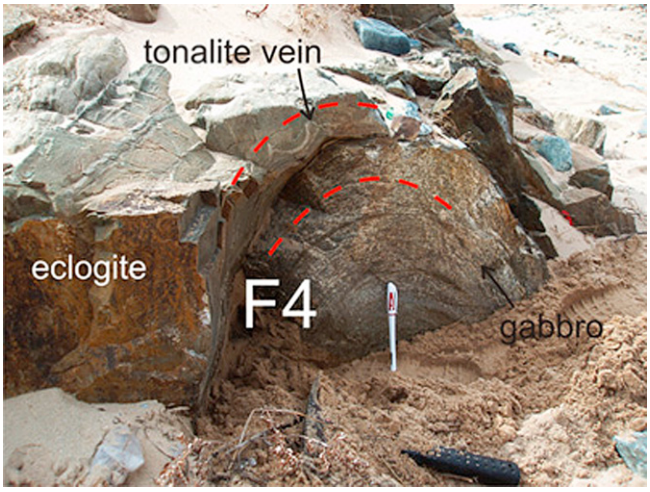

Fig. 10. Tonalite intruded after F_2 and before F_4. The fold shown is an F_4 fold, with gabbro in the core and eclogite on the outer edge of the outcrop. A thin tonalitic vein in the eclogite is an apophysis from a larger tonalite sheet that intrudes the edge of the outcrop, and it cuts the S_2 foliation associated with F_2, but is folded along with the S_2 foliation by the F_4 fold.

of garnet + amphibole + rutile/ilmenite. In this stage, most of omphacite and garnet grains were altered and only small relics are preserved. Most omphacite grains are retrogressed into amphibole and chlorite, and large garnet crystals are rare. Some fine grained garnet is present around altered omphacite, indicating possible recrystallization of garnet (Fig. 4h).

Most of the eclogites have a moderately strong foliation (S_4) which preserves the eclogite at lower strains than in the surrounding mylonites. Zircon U–Pb SHRIMP dating indicate that the protolith and UHP metamorphic age of the Yangkou UHP eclogite are within the ranges of 690–780 Ma, and 240–405 Ma respectively (Zheng et al., 2004; Katsube et al., 2008).

3.1.2. *Quartzo-feldspathic gneiss and mafic-ultramafic boudins*

The UHP eclogitic assemblages at Yangkou Bay are exposed in a structural window (Fig. 3), separated by a mylonitic detachment surface from surrounding amphibolite facies layered gneiss with mafic-ultramafic boudins. There are also thin slices of the gneiss tectonically interleaved with the western part of the eclogite body, but too thin to show on the map. The gneiss shows amphibolite and greenschist facies overprinting but also preserves evidence for UHP metamorphism since coesite inclusions occur in zircon from the country rock gneisses (Ye et al., 2000b). A penetrative schistosity (S_3) is defined by shape-preferred orientation of fine-grained quartz, feldspar, biotite, and amphibole, which is parallel to the compositional layering of the gneiss. Some layers are composed completely of medium grained quartz bands. In some areas (e.g., location A-1 in Fig. 3), the quartzo-feldspathic gneiss shows augen structures, with potassium feldspar phenocrysts surrounded by plagioclase and white mica tails (Fig. 5a).

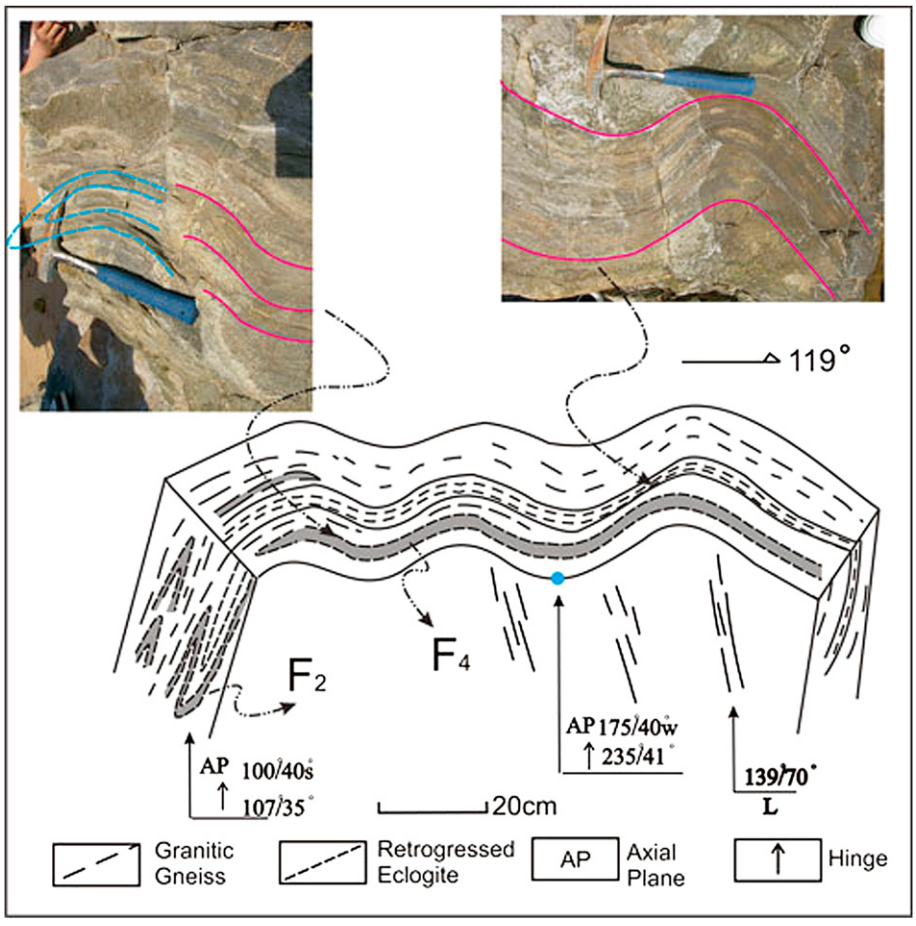

Fig. 11. F_2 fold overprinted by F_4 fold in retrogressed eclogite. Field photographs show structural relationships from areas indicated by arrows.

Melanocratic boudins preserved in the UHP gneiss include several large mafic-ultramafic lenses, one large boudenaged layer of quartz-biotite schist (interpreted as metapelite; Location B-2 in Fig. 3), two retrogressed eclogite bodies (Location C-3 in Fig. 3) and many small lozenges of mica schist (Location D-4 in Fig. 3). The mica schist boudins have a dark green color, and are mostly composed of coarse grained mica with amphibole and chlorite. Compositional layering and foliation is parallel to that of the country rock quartzo-feldspathic gneiss, and deformed together with the gneiss.

3.1.3. Tonalitic gneiss

There are two small dikes and plugs of tonalitic gneiss that cut across F_1 and F_2 folds (and S_1 and S_2 foliations) in the Yangkou eclogite, but contain the younger S_3 and S_4 fabrics in the eclogite. These S_3–S_4 fabrics are the same as the S_3–S_4 foliation in the quartzo-feldspathic gneiss. Detailed discussion of these relationships is provided in the structural sequence description below (Section 4.1). The tonalitic gneiss has an intrusive contact with the UHP unit and ultramylonite. The rock has a light grey color, is coarse grained, and its mineral composition assemblage is quartz + biotite + feldspar + amphibole. It is strongly lineated and has well developed joints.

3.1.4. Granitic, quartz porphyry dikes, felsite, lamprophyre dikes

The eclogite and eclogite mylonite are cut by a large late (circa 130–100 Ma, Zhao et al., 1998; Guo et al., 2002) pink-colored quartz porphyry dike (Fig. 3), exhibiting a fine grained matrix with fine-medium grained quartz phenocrysts. Its mineral assemblage includes dominantly quartz, feldspar, and magnetite. It intruded the quartzo-feldspathic gneiss as a dike striking roughly E–W (100°) and shows no strong ductile deformation but exhibits a broad open fold. Three groups of joint systems are well developed in the dike.

Many light grey felsite veins crop out adjacent to the serpentinized peridotite boudins within the quartzo-feldspathic gneiss. They have a much finer grain size than the quartz porphyry and are mostly composed of fine-grained twinned plagioclase feldspar (85%) and quartz (15%).

The outcrop is cut by two small lamprophyric dikes in the central and eastern parts of the area (Fig. 3). Both dikes are about 80–120 cm wide, with abundant phenocrysts of plagioclase feldspar, olivine, pyroxene, and amphibole (comprising 50% of the rock) in a fine-grained biotite-rich matix, and are not obviously deformed. Similar lamprophyre dikes across the Shandong Peninsula are dated to be Cretaceous (110 Ma) in age (Qiu et al., 2001; Yan and Chen, 2007).

3.2. Shear zones

Shear zones are best-preserved in central area 1 (Fig. 3). Several generations of folded shear zones are present, both in foliated eclogite and quartzo-feldspathic gneiss.

3.2.1. Quartzo-feldspathic mylonite

Quartzo-feldspathic mylonites mostly crop out at the western end of the main outcrop (Area 1, Fig. 3) at Yangkou, previously mapped (Zhao et al., 2005) as heterogeneous granitoid mylonite.

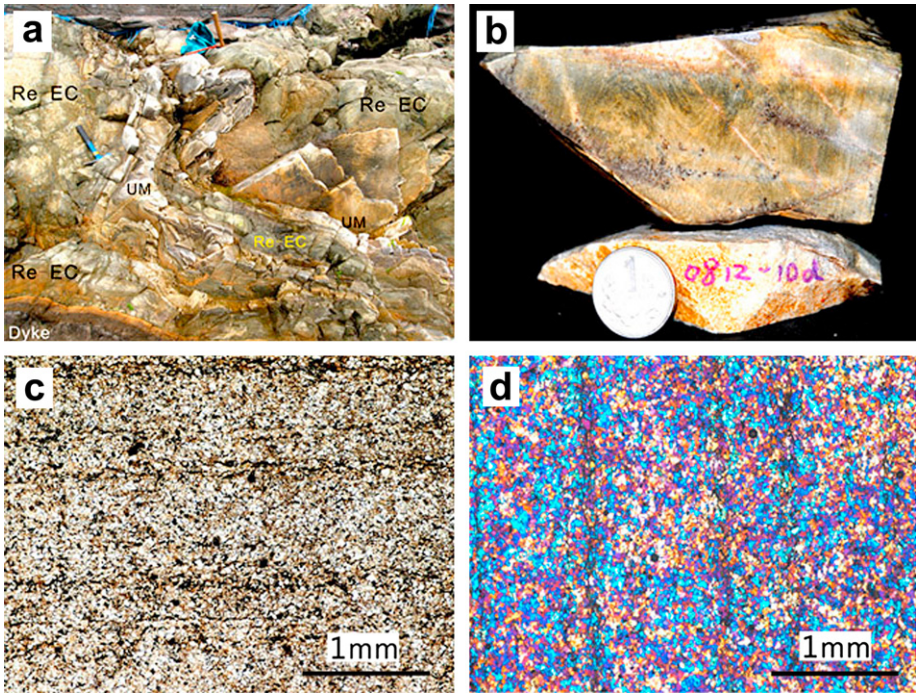

Fig. 12. Field photo, hand specieman and photomicrographs of the ultramylonite in Yangkou (Re–Ec: retrogressed eclogite, UM: ultramylonite). (a) Ultramylonite is folded together with eclogite at outcrop scale, camera lense facing to the north. Grey layers are ultramylonite and yellow-green parts are eclogite. A clear interlayered relationship is shown in the outcrop between ultramylonite and eclogite. Both the ultramylonite and eclogite are folded together (fold hinge plunging to the south west) and overprinted by different stages of folds. From outcrop scale, isoclinal folds are shown in retrogressed eclogite, however isoclinal folds are also exhibited on certain planes of the ultramylonite (Fig 12b). Strong foliation and lineation (dipping to the south) developed in the folded ultramylonite, lineation defined by greenschist facies minerals such as mica and chlorite are not folded by ultramylonite and eclogite, indicating a later greenschist facies deformation event. Left lower corner of this outcrop is cut by a late lamprophyre dyke striking EW. (b) Ultramylonite hand specimen sample showing clear tight-to isoclinal folds in some layers, and strong mylonitic foliation in other layers. At least two stages of folds (isoclinal F3 fold and similar shape F4 fold) displayed in this sample and overprinted by a later stage of foliation. (c) Photomicrograph of quartzo-feldspathic ultramylonite, plane-polarized light. In between the quartz ribbons, dark minerals are chlorite and mica, plus minor magnetite + pyrite. Most of quartz grains are very fine grained and statically recrystallized. (d) Phtomicrograph of ultramylonite under cross-polars with gypsum plate (530 γm). The blue grains show linear banded quartz ribbons which has a clear shape-preferred orientation parallel to the lineation, and the dominant blue colors indicate a strong lattice preferred orientation. Static-dominated recrystallization as well as dynamic recrystallization of quartz grain boundaries are both displayed.

This mylonite has a light grey color, strong foliation and well-developed lineation. The main mineral composition is quartz + plagioclase + biotite + zoisite, and the protolith is close to tonalite in mineralogy. The quartzo-feldspathic mylonites bound the UHP unit and are locally interlayered with gabbroic eclogite, and retrogressed eclogite, all of which are folded together (Figs. 3 and 5b).

3.2.2. Eclogite mylonite

The eclogite mylonite is preserved as a variably-thick zone, generally 5 cm–50 cm wide, that separates different eclogite layers from each other, and separates the eclogite from the surrounding gneiss (Figs. 3 and 5b). In the eclogite mylonite, most of the UHP phases are plastically deformed and define a strong eclogite facies foliation. Omphacite is dynamically recrystallized to fine grains defining an elongated shape fabric (lineation) within the foliation, while garnet is typically fractured with little plastic deformation. The recrystallized grains show a significant grain size reduction. Their long grain boundaries have smooth contacts with their neighbors and are parallel to the mylonitic foliation, whereas their short grain boundaries are typically serrated or sutured and orientated at high angles to the foliation. Porphyroclasts of omphacite are rarely preserved and show a core-mantle structure in the samples studied.

4. Structural sequence

The Yangkou Bay area is a complex multiply-metamorphosed and deformed UHP terrain where some of the highest-pressure metamorphic rocks in the Dabie-Sulu orogen are cut by several generations of igneous melts, including a late 130–100 Ma dike. Fortunately, in this location, outcrops at low tide preserve relationships between metamorphic and deformational processes. This has enabled us to accurately define the structural framework, necessary to define the sequence of structural events and processes associated with the subduction and then exhumation of these UHP rocks from lower to upper crustal levels. Understanding the structural history makes it possible to put metamorphic samples into a structural context and understand the link between deformation and metamorphism and place constraints on the metamorphic processes involved in the exhumation process. The main contribution of this paper is to provide accurate and precise maps that demonstrate relationships between different units, examine and compare the internal structural histories of each fault-bounded nappe, assess the protoliths of the different rock units involved, and provide a framework for discussion of different metamorphic and structural process involved in the tectonic events associated with the formation of UHP terrains. The mapping also provides a basis of future metamorphic and structural studies focused on these processes.

Figs. 3, 6 and 7 show the detailed mapping based on a high-resolution GPS web built on a 1:200 survey grid (conducted by Laoshan National Park for this project), supplemented with high-resolution ETM + Landsat and SPOT imagery, so the maps we present here are geographically accurate and internally precise, enabling the geometries of structures to be accurately portrayed.

The structural maps and cross-section (Figs. 3, 6 and 7) show that the study area is composed largely of quartzo-feldspathic gneiss, in which UHP metamorphic igneous rocks and their

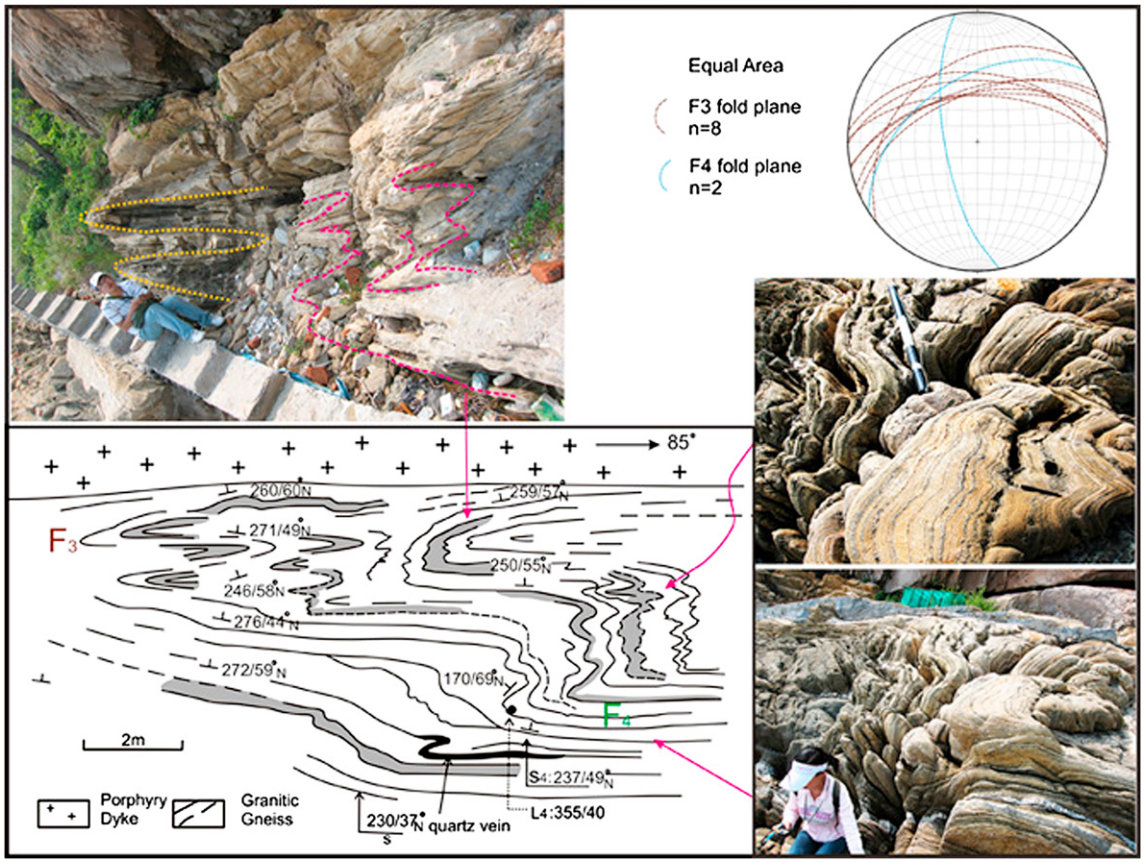

Fig. 13. F_3 fold overprinted by F_4 fold in quartzo-feldspathic gneiss. Field photographs show structural relationships from areas indicated by arrows, and lower-hemisphere equal area projection shows orientations of F_3 and F_4 folds on this outcrop. From location E5 on Fig. 3.

metamorphic equivalents crop out, and show complex fold interference patterns.

The eclogite units are deformed by F_1 early rootless isoclinal folds, F_2 and F_3 isoclinal fold nappes bounded by mylonites, that are also correlated with similar folds in surrounding quartzo-feldspathic gneiss, F_4 open folds about E-W to NW axes, and late F_5 warps about NS axes (Figs. 6 and 7). The early F_1 and F_2 folds are overprinted by amphibolite and greenschist facies metamorphic fabrics and S_2–S_4 shear zones that become wider and more pervasive with decreasing metamorphic grades.

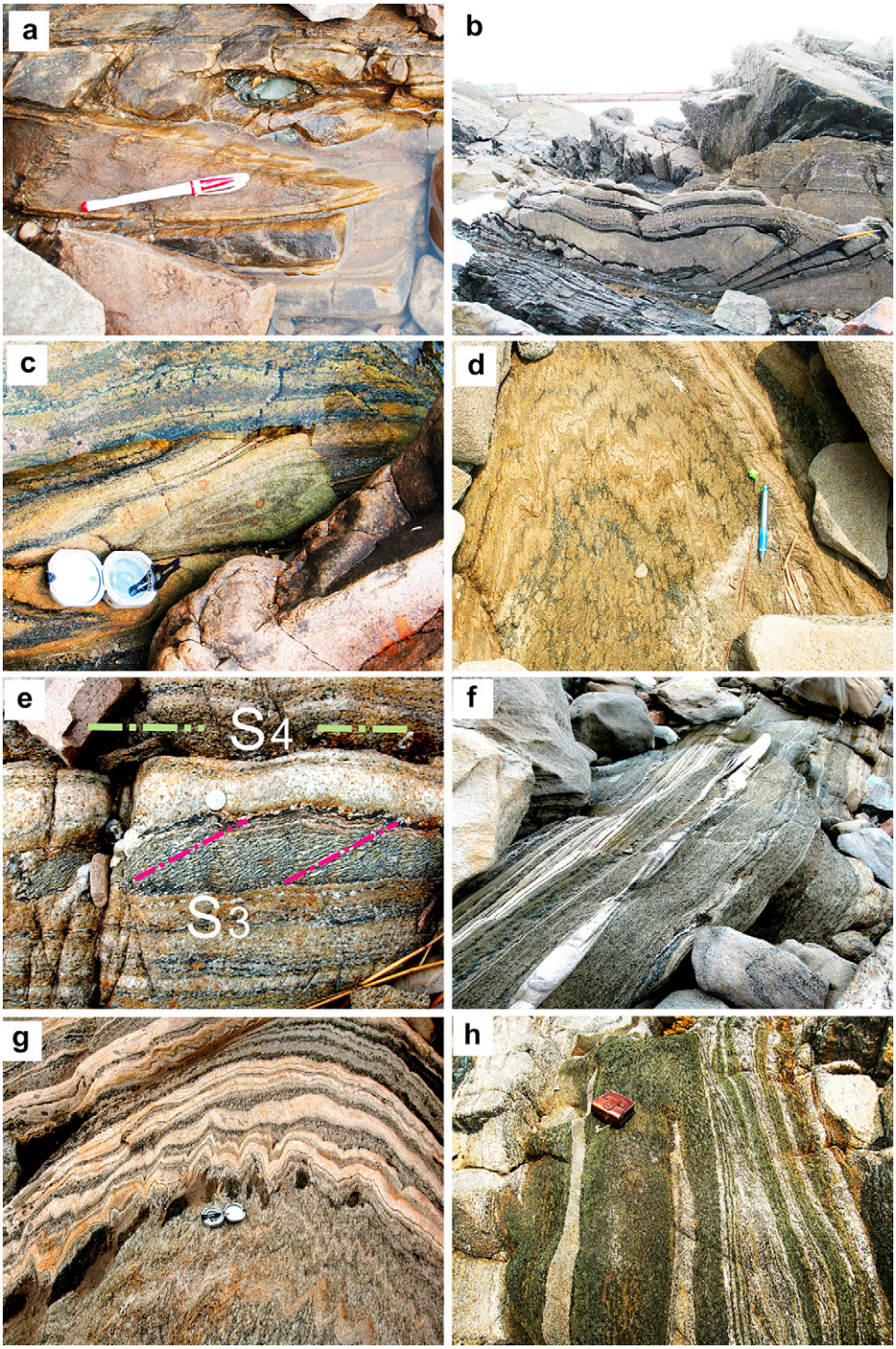

Fig. 14. (a) Isoclinal F_3 folds in quartzo-feldspathic gneiss; (b) Isoclinal recumbent F_3 fold; (c) F_3 Sheath fold; (d) F_4 and crenulation lineation (L_4); (e) S_3 foliation transposed by S_4 in quartzo-feldspathic gneiss on limb of F_4 fold in detailed map area 2 (Fig. 7); (f) F_3 isoclinal fold on limb of F_4 fold in detailed map area 2 (Fig. 7); (g) cuspate – lobate folds in hinge of F_4 fold in detailed map area 2 (Fig. 7); (h) metapelite unit (at location 4D on Fig. 7) showing S_3 and S_4 foliations.

4.1. Eclogite facies deformation: F_1 and F_2

Eclogite facies fabrics (S_1 and S_2) are locally well-preserved in relatively weakly deformed zones such as early fold hinges, where statically recrystallized garnet and omphacite are aligned with a weak preferred orientation (Fig. 5c). This type of fabric might represent an upper mantle flow structure (e.g., Vissers and Nicolas, 1995; Nicolas, 1989) or could be the original layers from the protolith deformed in the UHP peak eclogite facies stage of metamorphism. Omphacite and garnet are relatively coarse grained, and coesite is preserved as inclusions and as intergranular grains in the tectonite, indicative of UHP deformation (Zhao et al., 2005). Phengite that formed during an early eclogite facies retrogression stage shows a different orientation (or no preferred orientation) than S_1 (Fig. 5d). This means S_1 formed before the phengite started to grow.

The first penetrative fabric (S_2) at Yangkou includes the mineral assemblage garnet + omphacite + phengite + rutile + quartz, interpreted as the second eclogite facies fabric. The quartz content of units with S_2 but no S_1 fabric is higher than the eclogite samples with S_0 preserved. Interestingly, a thin layer of coronas started to grow on the omphacite; symplectite minerals including hornblende and albite are very fine grained. Garnet, omphacite, phengite and rutile show a clear preferred orientation, defining S_2 and L_2 (Fig. 5e and f). Garnet shows evidence for dynamic recrystallization including formation of subgrains visible in EBSD imagery and plastic deformation of omphacite is also shown by the formation of new subgrains (Zhao et al., 2003, 2005). This fabric represents the early stage of exhumation of eclogite from upper mantle depths, and still belongs to eclogite facies deformation, even though it is a retrograde metamorphism from the coesite stability field to the quartz-eclogite field during an early stage of exhumation.

Two eclogite facies fold generations were mapped within UHP eclogite units. The earliest F_1 consists of rootless isoclinal folds within foliated eclogite (S_1) (Fig. 8). These folds have extremely attenuated limbs and typically consist of isolated elongate hinges. The matrix is foliated eclogite and normally overprinted by amphibolite facies S_2 retrogression fabrics. These early folds in the basaltic and gabbroic eclogite could have formed during the prograde metamorphic path, during the initial subduction of the UHP unit. The prograde path is also recorded in the gabbro to eclogite transition in the UHP unit (Zhang and Liou, 1997).

Some F_2 isoclinal folds are bounded by mylonites, and also present in surrounding quartzofeldspathic gneiss. Most of these eclogite folds have nearly vertical fold axial planes (Figs. 9–11).

4.1.1. Ultramylonites

Mylonitic to ultramylonitic shear zones separate several small-scale 5–10-m-thick nappes of ultramafic-mafic UHP rocks, banded quartzo-feldspathic gneiss, and mafic lenses at Yangkou Bay (Fig. 6).

Fig. 12 shows detailed field, hand sample, and photomicrographs of this ultramylonite. On the field scale the ultramylonite is folded together with the eclogitic units and defines its contact with the quartzofeldspathic gneiss (Figs. 3, 6 and 12a). In cut slabs, the ultramylonite exhibits an intensely strong foliation (Fig. 12b), which in some places is folded and overprinted by younger foliations and lineations. Viewed in thin section, it is apparent that the ultramylonite has experienced late static recrystallization as most quartz grains are recrystallized into equant grains that meet at 120° triple junctions (Fig. 12c). However, a strong crystallographic preferred orientation is preserved as shown by the common crystallographic orientation revealed using a gypsum plate (Fig. 12d), and by quartz ribbons oriented parallel to the lineation.

Table 1
Table showing correlation of structural, metamorphic, and igneous events in the Yangkou Bay UHP map area.

Deformation sequence	Type of fabric		Fabric orientation	Related structure (shearzone, folds)	Axial plane orientation	Metamorphic conditions	Igneous activity
D0	S0	Grt + Cpx + Pl + Qtz	Variable, folded	Gabbroic structure with relic magmatic structure	Variable, folded	Granulite-facies	
D1	S1	L1: Grt + Omp, weak SPO	Variable, folded	F_1, rootless isoclinal eclogite folds	Variable, folded	UHP Eclogite facies	
D2	S2	L2: Grt + Omp + Ru + Phg; strong LPO, SPO mylonite (gabbroic eclogite); ultramylonite	Variable, folded	F_2, isoclinal eclogite folds (possibly same as F_3 in gneiss)	Steep, variable, folded	HP Eclogite facies	
	S2	Aligned amphibole in foliation intensification zone			Variable, folded	High amphibolite facies	
						High amphibolite facies	Foliated tonalite Intrusion (between granitoid-gabbro gneiss, eclogite and ultramylonite)
D3	S3	L3: Grt + Hb + Ru + Bt; Hb + Pl; Pl + Qtz + Zo + Bt	NE	F_3, Isoclinal folds (possibly same as F_2 in eclogite)	EW–NE	Amphibolite facies	
D4	S4	L4: Pl + Qtz + Chl + Bt	EW-NE	F_4 open folds	EW–NW	Greenschist facies	
				Extensional intrusion			Quartz porphyry dykes
D5	S5	Pl + Qtz + Chl + Bt	NS-NW	F_5 warps of fold + Cretaceous dykes	NS	Greenschist facies	
D6				Brittle deformation (3 joint sets in quartz porphyry dykes)			

SPO – shape-preferred orientation; LPO – lattice preferred orientation.

4.1.2. Tonalite intrusion and deformation

There are several small dikes and plugs of tonalite that cut across early fabrics in the Yangkou eclogite, but contain the younger fabrics (S_3 and S_4), and thus could be used to place limits on the ages of these fabrics. One small tonalite plug (smaller than map scale) intruded along the contact between the banded granitoid-gabbro gneiss and ultramylonite (location A2, Figs. 3 and 6), and is strongly lineated, and has well-developed joints. Near the western end of the outcrop area, a refolded amphibolite facies (retrogressed eclogite) knob shows that the tonalite intruded after F_2 and before F_4 (Fig. 10).

4.2. Amphibolite – greenshist facies deformation

4.2.1. Amphibolite facies deformation, F_3

Large areas of Yangkou Bay are comprised of amphibolite, largely retrogressed from eclogite. S_3 in amphibolite is defined by oriented mica and amphibole, while in lighter colored quartzo-feldspathic gneiss, it is mainly defined by stretched quartz and feldspar. This foliation is widely developed in the country rock of the UHP rocks, dipping NW, parallel to its compositional layering S_0 and composite S_1 and S_2 foliations (Figs. 6 and 7). Dark mafic layers and amphibolites are stretched into lenses and ultimately, into thin layers parallel to S_1 and S_3.

F_3 folds are defined by original compositional layers and the regional S_2 foliation that are both folded and deformed into tight isoclinal folds (Figs. 13 and 14a). They are well-preserved with compositional differentiation parallel to the axial surfaces, which are almost vertical, striking ~135°. The folds are broadly similar in style but typically with one attenuated limb, and sub-angular hinges, falling between Ramsay Class II and Class III folds. In the eastern part of the area (Fig. 7) F_3 folds have been rotated into parallelism with F_4 folds, and the F_3 fabrics (S_3) are locally transposed by F_4 fabrics (S_4). In this area, F_4 fold hinges preserve remnants of S_3 as oblique differentiated layers with rare isoclinal fold hinges in the more pelitic units (Fig. 14e), forming a classic transposed foliation (e.g., Borradaile et al., 1982; Sander, 1911, 1930; Turner and Weiss, 1963; Williams, 1983).

In some cases, F_3 is manifested as isoclinal recumbent folds with axial surfaces parallel to the granitic and eclogitic mylonite foliation (Fig. 14b). The hinges are curved and close to horizontal, trend SE, and have shapes characteristic of Ramsay Type IC folds (Fang and

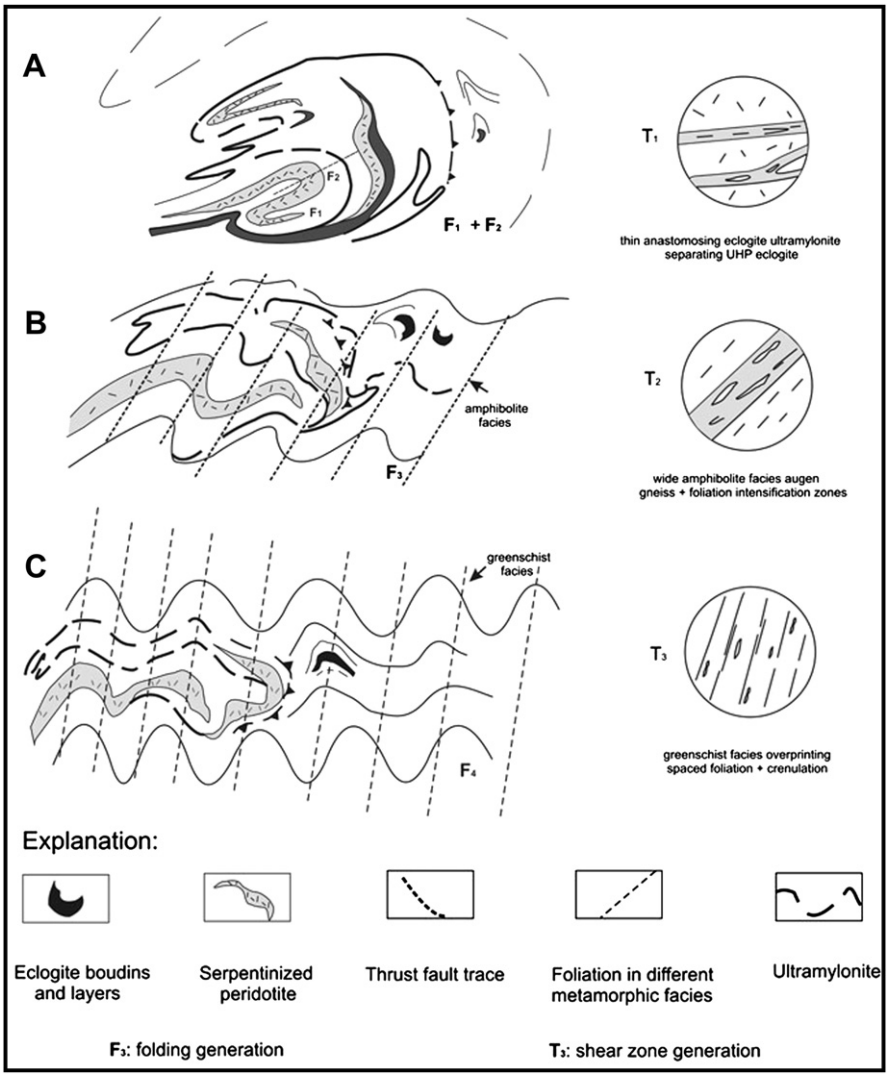

Fig. 15. Progressive deformation model of Yangkou UHP rocks and shear zone. (A) F_1 and F_2 folds and associated foliations are formed at UHP eclogite facies conditions, and include the development of narrow ultramylonitic shear zones, as the eclogite body is rolled into a refolded nappe. (B) shows overprinting by wider amphibolite facies shear zones and retrogressive shear zones, and (C) shows the overprinting by regional greenschist facies fabrics. This deformation sequence formed during the progressive retrograde path of the eclogite as it was brought from ~200 km to the surface.

Zhao, 2004). In some other cases, thin layers of granitic mylonite are folded into sheath folds (Fig. 14c). Further work is needed to determine if F_3 folds have curved hinges because they are folded, because they were superimposed on top of asymmetric F_2 folds, or because of high shear strains as in sheath folds.

4.2.2. F_4 greenshist facies deformation and metamorphism, overprint on F_3

Greenshist facies deformation and metamorphism widely overprints the granitoid gneiss. F_3 is refolded by F_4 which shows more angular fold styles and has fabrics developed together with greenschist facies retrogression. In the hinge regions, crenulation lineations surround the F_3 fold axes, displaying cuspate-lobate patterns (Fig. 14d and f) at the contacts where there is a strong competence contrast (e.g., Ramsay and Huber, 1987) between quartz and mica rich layers. On these cleavage planes, biotite and chlorite minerals show that F_4 structures developed during greenshist facies deformation.

In some cases, greenschist facies metamorphism and deformation are overprinted on both interlayered granitoid gneiss and retrogressed amphibolite facies eclogite layers. Isoclinal recumbent F_3 folds are refolded by open folds (with a nearly box fold style). F_4 folds (Figs. 6 and 7) with axial surfaces striking EW to NW (153°) and dipping moderately SW (53°W) exhibit a new greenshist facies foliation (S_4) that displaces the S_3 amphibolite facies foliation forming a crenulation foliation.

F_5 warps older layers about NS axes (Figs. 6 and 7) and formed at shallow depths of deformation. This very late phase of deformation is mostly shown by the quartzo-feldspathic gneiss and in Cretaceous dykes such as quartz porphyry that cut the area.

5. Tectonic interpretation and implications for continental collision tectonic processes

Well-preserved structural and igneous relationships at Yangkou Bay were mapped in detail (1:200–1000) to define the structural geometry and history of the UHP rocks (Table 1). Quartzo-feldspathic gneiss with enclaves of UHP mafic igneous rocks exhibit complex fold interference patterns. High-precision mapping of key areas shows that eclogite mylonites are re-folded by at least two generations of post-eclogite folds (Table 1). The eclogite units are deformed by F_1 early rootless isoclinal folds, F_2 and F_3 isoclinal fold nappes bounded by mylonites, that are also present in surrounding quartzo-feldspathic gneiss, F_4 open folds about E-W to NW axes, and late F_5 warps about NS axes (Table 1). The early folds are overprinted by amphibolite and greenshist facies metamorphic fabrics and shear zones that become wider and more pervasive with decreasing metamorphic grades.

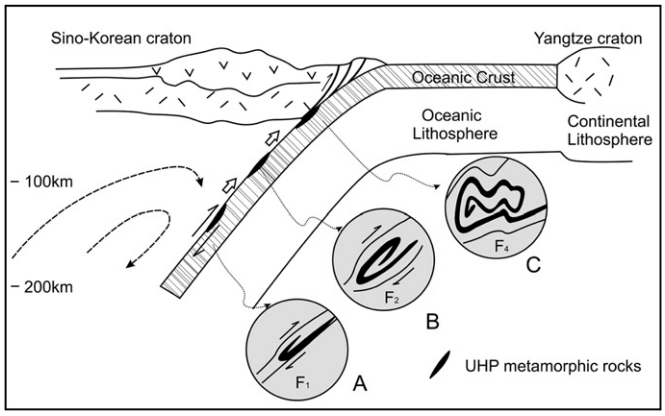

Fig. 16. Tectonic model for the subduction and exhumation process of the Yangkou UHP rocks. We suggest a model in which the eclogite body was detached from the down-going plate at location A, and then experienced two isoclinal folding episodes at UHP eclogite facies conditions as the rocks were rolled along the subduction channel from ~200 to 120 km depth. Successive deformation events occurred as the eclogite body was juxtaposed with the quartzo-feldspathic gneisses, and exhumed to the surface.

The sequence of deformation and metamorphism documented in Yangkou provides a unique example of the complex interplay between deformational and metamorphic processes associated with the initial subduction of rocks formed near the surface, and their later exhumation as UHP metamorphic rocks from mantle depths of ~200 km to upper crustal levels. Early UHP structures are dominated by thin anastomosing ultramylonitic shear zones separating internally re-folded nappes which form jelly-roll like structures at scales of tens of meters (Fig. 15a). The prograde history is partly preserved in the center of the UHP block where the gabbro to eclogite transition is documented (e.g., Zhang and Liou, 1997), and the early F_1 rootless isoclinal folds in the basaltic eclogite may also be related to the prograde, or subduction stage of the collision. These internally rolled up nappes were initially thin slices of a circa 750–800 Ma old mafic basalt-gabbro-peridotite series that were derived from either the down-going subducting plate or the overriding plate and brought to depths of 200 km, then rolled along the boundary between the two colliding plates during the collision of the North and South China cratons 240 million years ago (Fig. 16). Interestingly, the circa 750–800 Ma protolith age for the eclogite suggests that the mafic/ultramafic sequence is the same age as oceanic lithosphere generated along with the break-up and dispersal of Rodinia (Katsube et al., 2008), and thus, the metabasalt, gabbro, and ultramafic rocks may represent a fragment of oceanic lithosphere. The zone along which the UHP rocks were internally re-folded (rolled) may have been quite thin, confined to the active boundary between the overriding and subducting plates in the subduction channel, in a thin zone of high vorticity induced by the high shear strains along the plate boundary, and the large rheological contrasts between the different rock units involved. Most of the observed deformational and metamorphic fabrics record a retrograde path (path A → B → C on Fig. 16) implying that the eclogite lenses were detached from the down-going plate at about 200 km depth, then progressively deformed during their retrograde near-isothermal decompression during ascent to the surface. It is less-likely that the eclogites were detached from the overriding plate, as they would need to be structurally removed from the base of the crust, then deformed and brought to 200 km depth on a prograde path before their eventual retrogression and deformation during ascent (path C → B → A → B → C on Fig. 16).

As the UHP rocks were exhumed to amphibolite facies conditions and tectonically emplaced into a continental-quartzo-feldspathic gneiss sequence, the next generation of overprinting structures were dominated by wider shear zones (Fig. 15b), zones of foliation intensification (FIZ's) and widespread retrogression of mineral and structural textures. The amphibolite facies structures are nearly pervasive, and show folds on scales of tens to hundreds of meters, with the FIZ's associated with inclined fold axial surfaces. Finally, as the rocks at Yangkou were uplifted into greenschist facies the metamorphism and retrogression became more zonal and spaced, with more upright folds that are more concentric in style (Fig. 15c) than the earlier amphibolite facies similar-style folds (Fig. 15b). This style is in contrast with the eclogite facies rootless isoclinal folds that became rolled into jelly-roll like nappes during deep crustal or upper mantle depths.

The change in deformation character from thin anastomosing shear zones formed at UHP conditions to wider more penetrative zones of deformation at higher crustal levels is one of the most salient features of the map pattern at Yangkou that may have

general applications to understanding lower crustal and upper mantle deformation (e.g., Jin et al., 2001; Zhang et al., 1996, 2006). The centimeter to decameter scale UHP ultramylonitic shear zones formed at 200–100 km depth separate 5–10 m wide lozenges of relatively low strain, showing that these shear zones were able to accommodate large strains and displacements between the structural slices on either side of the shear zones. This in turn implies that once strain is localized and initiated at one location under UHP conditions that crystallographic deformation mechanisms operate efficiently and are able to accommodate any imposed strain. In contrast, at lower PT conditions characteristic of lower grades of deformation, the shear zones become wider, and the strain more penetrative, showing that strain localization mechanisms are less-efficient at higher crustal levels. It is possible that at lower PT conditions, fewer slip systems in the host minerals are able to be activated, and to accommodate a general strain the width of the deforming zone needs to be wider. Further work on the crystallographic deformation mechanisms is needed to address these questions. While Yangkou is just one example preserving contrasting deformation mechanisms across a wide range of crustal and upper mantle conditions, it preserves one of the most complete records of deformation and metamorphism from shallow crustal levels, then subduction to 200 km depth, then back to near surface conditions. The links between the structural sequence and metamorphic history at Yangkou make this a natural laboratory and museum for testing present and future models of the exhumation processes associated with forming one of geology's most unusual occurrences of UHP minerals, metamorphic assemblages, and deformation fabrics.

Acknowledgements

We thank Liang Zhao, Ruirui Wang, Weihong Yang, Weili Dong, Xiangjun Cong, Xuya Huang from SRTP (Student Research Training Project) group in Ocean University of China for data collection and mapping on outcrops, Dr. Abuduwasit Ghulam from Saint Louis University for Remote Sensing and GIS technical support. Mr Guo Liang and Xiang Shibao are thanked for arranging logistical support and surveying in Laoshan National Park, and supporting these scientific studies. Financial support was provided by National Science Foundation of China (NSFC Grant 40802045), Science Foundation of Shandong Province, China (Grant Q2008E03), the National Natural Science Foundation of China (Grant 40821061) and the Ministry of Education of China (B07039). Special appreciation to very helpful comments from two reviewers, Simon Wallis and Domingo Aerden.

References

Ames, L., Zhou, G., Xiong, B., 1996. Geochronology and geochemistry of ultrahigh-pressure metamorphism with implications for collision of the Sino-Korean and Yangtze cratons, central China. Tectonics 15, 472–489.

Ames, L., Tilton, G.R., Zhou, G., 1993. Timing of collision of the Sino-Korean and the Yangtze cratons: U–Pb zircon dating of coeiste-bearing eclogites. Geology 21, 339–342.

Baldwin, S.L., Webb, L.E., Monteleone, B.D., Little, T.A., Fitzgerald, P.G., Chappell, J.L., 2005. Metamorphism and Exhumation of the Youngest Known HP/UHP Terrane on Earth, Eastern Papua New Guinea. American Geophysical Union. Fall Meeting Abstract #V54B-01.

Borradaile, G.J., Bayly, M.B., Powell, C.McA., 1982. Atlas of Deformational and Metamorphic Rock Fabrics. Springer-Verlag, Berlin, 551 pp.

Brown, M., Piccoli, M., 2006. Granulites and Granulites. Abstracts of Meeting, Brasilia, July 10-12, 2006.

Brown, M., Rushmer, T., 2006. Evolution and Differentiation of the Continental Crust. Cambridge University Press, Cambridge.

Brueckner, H.K., van Roermund, H.L.M., 2004. Dunk tectonics: a multiple subduction/eduction model for the evolution of the Scandinavian Caledonides. Tectonics 23, TC2004. doi:10.1029/2003TC001502.

Chemenda, A.P., Matte, V., Sokolov, V., 1997. A model of Palaeozoic obduction and exhumation of high-pressure/low-temperature rocks in the southern Urals. Tectonophysics 276, 217–227.

Cheng, Y.Q., Liu, D.Y., Willimas, I.S., Jian, P., Zhuang, Y.X., Gao, T.S., 2000. SHRIMP U–Pb dating of zircons of a dark-colored eclogite and a garnet-bearing gneissic-granitic rock from Bixiling, eastern Dabie area, Anhui Province: isotope chronological evidence of Neoproterozoic UHP metamorphism. Acta Geologica Sinica 74, 748–765.

Chopin, C., 1984. Coesite and pure pyrope in high-grade blueschists of the western Alps – a 1st record and some consequences. Contributions to Mineralogy and Petrology 86 (2), 107–118.

Chopin, C., 2003. Ultrahigh-pressure metamorphism: tracing continental crust into the mantle. Earth and Planetary Science Letters 212, 1–14.

Fang, A.M., Zhao, Z.Y., 2004. The constituents of the Qingdao Yankou high to ultrahigh-pressure tectonic mélange and their deformations. Acta Petrological Sinica 20 (5), 1087–1096 (in Chinese with English Abstract).

Faure, M., Lin, W., Monié, P., Breton, N.L., Poussineau, S., Panis, D., Deloule, E., 2003. Exhumation tectonics of the ultra high-pressure metamorphic rocks in the Qinling orogen in E. China. New petrological-structural-radiometric insights from the Shandong Peninsula. Tectonics 22 (3), 1018. doi:10.1029/2002TC001450.

Guo, J.H., Chen, F.K., Zhang, X.M., Cong, B.L., 2002. Evolution of syn- to post-collisioinal granitoids from Sulu UHP belt, eastern China: zircon U-Pb geochronology and petrochemistry. In: International Workshop on Geophysics and Strucutral Geology of UHPM Terrains, pp. 92.

Hacker, B.R., Ratschbacher, L., Liou, J.G., 2004. Subduction, collision and exhumation in the ultrahigh-pressure Qinling-Dabie orogen. In: Geological Society of London, Special Publication, vol. 226 157–175.

Hacker, B.R., Ratschbacher, L., Webb, L., Ireland, T., Walker, D., Dong, S.W., 1998. U/Pb zircon ages constrain the architecture of the ultrahigh-pressure Qinling-Dabie Orogen, China. Earth and Planetary Science Letters 161 (1–4), 215–230.

Hacker, B.R., Ratschbacher, L., Webb, D., Dong, S.W., 1995. What brought them up? exhumation of the Dabie Shan ultrahigh- pressure rocks. Geology 23 (8), 743–746.

Hacker, B.R., Wallis, S.R., McWilliams, M.O., Gans, P.B., 2009. $^{40}Ar/^{39}Ar$ constraints on the tectonic history and architecture of the ultrahigh-pressure Sulu orogen. Journal of Metamorphic Geology 27 (9), 827–844.

Hacker, B.R., Wallis, S.R., Ratschbacher, L., Grove, M., Gehrels, G., 2006. High-temperature geochronology constraints on the tectonic history and architecture of the ultrahigh-pressure Dabie-Sulu Orogen. Tectonics 25, TC5006. doi:10.1029/2005TC001937.

Hirajima, T., 1996. Effect of jadeite-content on the garnet–clinopyroxene geothermometer for an ultrahigh-pressure eclogite complex. Proceedings of the Japan Academy, Series B 72, 249–254.

Hirajima, T., Wallis, S.R., Zhai, M., Ye, K., 1993. Eclogitized metagranitoid from the Sulu ultra-high pressure province, eastern China. Proceedings of the Japan Academy Series B 69 (No. 10), 249–254.

Hu, F.F., Fang, H., Yang, J.H., Wang, Y.S., Liu, D.Y., Zhai, M.G., Jin, C.W., 2004. Mineralizing age of the Rushan lode gold deposit in the Jiadong Peninsula: SHRIMP U–Pb dating on hydrothermal zircon. Chinese Science Bulletin 49, 1629–1636.

Hwang, S.L., Yui, T.F., Chu, H.T., Shen, P., Shertle, H., Zhang, R.Y., Liou, J.G., 2007. On the origin of oriented rutile needles in garnet from UHP eclogites. Journal of Metamorphic Geology 25, 349–362.

Jahn, B.M., 1998. Geochemical and isotopic characteristics of UHP eclogites and ultramafic rocks of the Dabie orogen. Implications for continental subduction and collision tectonics. In: Hacker, B., Liou, J.G. (Eds.), When Continents Collide. Geodynamics and Geochemistry of Ultrahigh-Pressure Rocks. Kluwer, Dordrecht, pp. 203–239.

Jin, Z.M., Zhang, J.F., Green II, H.W., Jin, S.Y., 2001. Eclogite rheology: implications for subducted lithosphere. Geology 29 (8), 667–670.

Katsube, A., Hayasaka, Y., Santosh, M., Li, S.Z., Terada, K., 2008. SHRIMP zircon U–Pb ages of eclogite and orthogneiss from Sulu ultrahigh-pressure zone in Yangkou area, eastern China. Gondwana Research 15 (2), 168–177.

Kusky, T.M., Santosh, M., 2009. The Columbia connection in North China. In: Geological Society of London, Special Publications, vol. 323 49–71.

Leech, M.L., Webb, L.E., Tang, T.N., 2006. Diachronous histories for the Dabie-Sulu orogen from high-temperature geochronology. In: Geological Society of America Special Paper, vol. 403 1–22.

Li, S.G., Sun, W.D., Zhang, Z.Q., Li, Q.L., 2001. Nd isotopic disequilibrium between minerals and Rb-Sr age of the secondary phengite in eclogite from the Yangkou area, Qingdao, eastern China. Chinese Science Bulletin 46, 252–255.

Li, S.Z., Kusky, T.M., Wang, L., Zhang, G.W., Lai, S.C., Liu, X.C., Dong, S.W., Zhao, G.C., 2007. Collision leading to multiple-stage large-scale extrusion in the Qinling orogen: insights from the Mianlue suture. Gondwana Research 12, 121–143.

Li, S.Z., Kusky, T.M., Liu, X.C., Zhang, G.W., Zhao, G.C., Wang, L., Wang, Y.J., 2009. Two-stage collision-related extrusion of the western Dabie HP-UHP metamorphic terranes, central China: evidence from quartz c-axis fabrics and structures. Gondwana Research 16, 294–309 (special issue).

Lin, W., Shi, Y.H., Wang, Q.C., 2009. Exhumation tectonics of the HP-UHP orogenic belt in Eastern China: new structural–petrological insights from the Tongcheng massif, Eastern Dabieshan. Lithos 109, 285–303.

Liou, J.G., Zhang, R.Y., 1996. Occurrences of intergranular coesite in UHP rocks from the Sulu region, eastern China: implications for lack of fluid during exhumation. American Mineralogist 81, 1217–1221.

Liou, J.B., Ye, K., Maruyama, S., Cong, B.L., Fan, H.R., 2001. Mineral inclusions in zircon from gneisses in the ultrahigh-pressure zone of the Dabie Mountain, China. Journal of Geology 109, 523–535.
Liu, F., Liou, J.G., Xu, Z., 2005. U–Pb SHRIMP ages recorded in the coesite-bearing zircon domains of paragneisses in the southwestern Sulu terrane, eastern China: new interpretation. American Mineralogist 90, 790–800.
Liu, D.L., Li, S.G., Ge, N.J., 1994. Journal of China University of Science and Technology. The three epoch deformation and tectonic significance of the Qingdao Yangkou tectonic mélange in collision zone of the North China Plate and the Yangze plate 24, 284–289 (in Chinese with English abstract).
Liu, D.Y., Jian, P., Kröner, A., Xu, S.T., 2006. Dating of prograde metamorphic events deciphered from episodic zircon growth in rocks of the Dabie–Sulu UHP complex, China. Earth and Planetary Science Letters 250, 650–666.
Maruyama, S., Liou, J.G., Zhang, R.Y., 1994. Tectonic evolution of the ultrahigh-pressure (UHP) and high-pressure (HP) metamorphic belts from central China. The Island Arc 3, 112–121.
Meng, Q.R., Zhang, G.W., 2000. Geologic framework and tectonic evolution of the Qinling orogen, central China. Tectonophysics 323, 183–196.
Molina, J.F., Austrheim, H., Glodny, J., Rusin, A., 2002. The eclogites of the Marun–Keu complex, Polar Urals (Russia): fluid control on reaction kinetics and metasomatism during high P metamorphism. Lithos 61, 55–78.
Nicolas, A., 1989. Structures of Ophiolites and Dynamics of Oceanic Lithosphere. Kluwer Academic Publishers, Boston.
Oh, C.W., Kusky, T.M., 2007. Review of the Late-Permian to Triassic Hongseong-Odesan Collision belt in South Korea and its tectonic correlation with Korea, China and Japan. International Geology Review 49, 636–657.
Okay, A.I., Sengor, A.M.C., 1992. Evidence for intracontinental thrust-related exhumation of the ultra-high-pressure rocks in China. Geology 20, 411–414.
Okay, A.I., Sengor, A.M.C., Satir, M., 1993. Tectonics of an ultrahigh-pressure metamorphic terrane: the Dabie-Shan Tongbai-Shan Orogen, China. Tectonics 12, 1320–1334.
Qiu, H.J., Xu, Z.Q., Zhang, J.X., Yang, J.S., Zhang, Z.M., Li, H.B., 2003. The discovery of glaucophane greenschist facies rock mass in Lianyungang, northern Jiangsu. Petrologica et Mineralogica 22, 34–40 (in Chinese with English abstract).
Qiu, J.S., Wang, D.Z., Luo, Q.H., 2001. $^{40}Ar-^{39}Ar$ dating for volcanic rocks of Qingshan Formation in Jiaolai Basin, Eastern Shandong Province: a case study of the Fenlingshan volcanic apparatus in Wulian County. Geological Journal of China Universities 7, 351–355 (in Chinese with English abstract).
Ramsay, J.G., Huber, I., 1987. The techniques of modern structural geology. In: Folds and Fractures, vol.2 2. Academic Press, Oxford. 292.
Ratschbacher, L., Hacker, B.R., 2000. Exhumation of the ultrahigh-pressure continental crust in east central China. Journal of Geophysical Research 105, 13303–13338.
Ratschbacher, L., Franz, L., Enkelmann, E., Jonckheere, R., Pörschke, A., Hacker, B.R., Dong, S.W., Zhang, Y.Q., 2006. The Sino-Korean–Yangtze suture, the Huwan detachment, and the Paleozoic–Tertiary exhumation of (ultra)high-pressure rocks along the Tongbai-Xinxian-Dabie Mountains. In: Hacker, B.R., McClelland, W.C., Liou, J.G. (Eds.), Ultrahigh-pressure Metamorphism: Deep Continental Subduction. Geological Society of America Special Paper, vol. 403, pp. 45–75.
Sander, B., 1911. Uber Zusammenhange Zwischen Teilbewegung und Gefuge in Gesteines. (On the Relationships Between Movement and Fabrics in Rock). Tshermaks Minerogie und Pterographie Mittelungen 30, 381–384.
Sander, B., 1930. Gefugekunde der Gesteine. Springer, Vienna (English Translation, An Introduction to the Study of Fabrics of Geological Bodies. Pergamon Press, Oxford, U.K.).
Smith, D.C., 1984. Coesite in clinopyroxene in the Caledonides and its implication for geodynamics. Nature 310, 641–644.
Sobolev, N.G., Shatsky, V.S., 1990. Diamond inclusions in garnets from metamorphic rocks. Nature 343, 732–746.
Song M.C., et al., 1984. Shandong Regional Geological Map, China Geological Survey Map, Scale 1:500,000.
Stefan, M.S., Bernhard, F., Eduard, K., Ralf, S., 2004. Tectonic map and overall architecture of the alpine orogen. Eclogae Geologicae Helvetiae 97, 93–117.
Suo, S.T., Zhong, Z.Q., You, Z.D., Zhou, H.W., 2000. Dynamics and relict UHP Structure in the Dabie-Sulu area. Earth Sciences 25, 557–563 (in Chinese with English abstract).
Turner, F.J., Weiss, L.E., 1963. Structural Analysis of Metamorphic Tectonites. McGraw Hill, New York.
Vissers, R.L.M., Nicolas, A., 1995. Mantle and Lower Crust Exposed in Oceanic Ridges and in Ophiolites. Kluwer Academic Publishers, Boston.
Wallis, S.R., Enami, M., Banno, S., 1999. The Sulu UHP terrane: a review of the petrology and structural geology. International Geology Review 41, 906–920.
Wallis, S.R., Ishiwatari, A., Hirajima, T., 1997. Occurrence and field relationships ultrahigh-pressure granitoid and coesite eclogite in the Sulu terrain, eastern China. Journal of the Geological Society 154, 45–54. London.
Wallis, S.R., Tsuboi, M., Suzuki, K., Fanning, M., Jiang, L., Tanaka, T., 2005. Role of partial melting in the evolution of the Sulu (eastern China) ultrahigh-pressure terrane. Geology 33, 129–132.
Wang, L., Jin, Z.M., Kusky, T., Xu, H.J., Liu, X.W., 2010. Microfabric characteristics and rheological significance of ultra-high-pressure metamorphosed jadeite-quartzite and eclogite from Shuanghe, Dabie Mountains, China. Journal of Metamorphic Geology 28, 163–182.
Webb, L.E., Leech, M.L., Yang, T.N., 2006. $^{40}Ar/^{39}Ar$ thermochronology of the Sulu terrane: Late Triassic exhumation of high- and ultrahigh-pressure rocks and implications for Mesozoic tectonics in east Asia. In: Geological Society of America Special Paper, vol. 403 77–92.
Wiesinger, M., Neubauer, F., Handler, R., 2006. Exhumation of the Saualpe eclogite unit, Eastern Alps: constraints from $^{40}Ar/^{39}Ar$ ages and structural investigations. Mineralogy and Petrology 88, 149–180.
Williams, P.F., 1983. Large scale transposition by folding in northern Norway. International Journal of Earth Sciences 72, 589–604.
Wu, Y.B., Zheng, Y.F., Zhou, J.B., 2004. Neoproterozoic granitoid in northwest Sulu and its bearing on the North China–South China blocks boundary in east China. Geophysical Research Letters 31, 1–4.
Xue, F., Rowley, D.B., Baker, J., 1996. Refolded syn-ultrahigh-pressure thrust sheets in the south Dabie complex, China: field evidence and tectonic implications. Geology 24, 455–458.
Yan, J., Chen, J.F., 2007. Geochemistry of Qingshan Formation volcanic rocks from Jiaolai Basin, eastern Shandong Province: Petrogenesis and geological significance. Geochemistry 36, 1–10 (in Chinese with English abstract).
Yang, T.N., Xu, H.F., Song, M.C., Zhang, J.X., 1997. Uplift-extension structure of the Jiaonan block. Geology of Shandong 13, 67–76.
Yang, W.C., 2002. Geophysical profiling of the Sulu ultra-high-pressure metamorphic belt, eastern China. International Workshop on Geophysics and Structure Geology of UHPM Terrains, pp. 8–11.
Ye, K., Hirajima, T., Ishiwatari, A., Guo, J., Zai, M., 1996. Finding of an intergranular coesite from Yangkou eclogite, Qingdao, and its significance. Chinese Science Bulletin 41, 1407–1408 (in Chinese).
Ye, K., Cong, B., Ye, D., 2000a. The possible subduction of continental material to depths greater than 200 km. Nature 407, 734–736.
Ye, K., Yao, Y., Katayama, I., Cong, B., Wang, Q.C., Maruyama, S., 2000b. Large area extent of ultrahigh pressure metamorphism in the Sulu ultrahigh pressure terrain of East China: new implications from coesite and omphacite inclusions in zircon of granitic gneiss. Lithos 52, 157–164.
Yoshida, D., Hirajima, T., Ishiwatari, A., 2004. Pressure–temperature path recorded in the Yangkou garnet-peridotite, in Su-Lu UHP metamorphic belt, eastern China. Journal of Petrology 45, 1125–1145.
Zhang, J.F., Green II, H.W., Bozhilove, K.N., 2006. Rheology of omphacite at high temperature and pressure and significance of its lattice preferred orientations. Earth and Planetary Science Letters 246, 432–443.
Zhang, G.W., Meng, Q.R., Yu, Z.P., Sun, Y., Zhou, D.W., Guo, L., 1996. Orogenesis and dynamics of the Qinling orogen. Science in China (Series D) 30, 225–234.
Zhang, R.Y., Liou, J.G., 1997. Partial transformation of gabbro to coesite-bearing eclogite from Yangkou, the Sulu terrane, eastern China. Journal of Metamorphic Geology 15, 183–202.
Zhang, R.Y., Liou, J.G., Cong, B., 2000. Petrochemical constraints for dual origin of garnet peridotites from the Dabie-Sulu UHP terrane, eastern-central China. Journal of Metamorphic Geology 18, 149–166.
Zhao, G.T., Wang, D.Z., Cao, Q.C., Yu, L.S., 1998. Thermal evolution and its significance of I–A type granitoid complex – the Laoshan Granitoid as an example. Science in China 41 (5), 529–536. English Version.
Zhao, Z.Y., Wei, C.J., Fang, A.M., 2005. Plastic flow of coesite eclogite in a deep continent subduction regime: microstructures, deformation mechanisms and rheologic implications. Earth and Planetary Science Letters 237, 209–222.
Zhao, Z.Y., Fang, A.M., Yu, L.J., 2003. High- to ultra-high pressure ductile shear zones in the Sulu UHP belt, eastern China. Terra Nova 15, 322–329.
Zheng, Y.F., Fu, B., Cong, B.L., Li, L., 2003. Stable isotope geochemistry of ultrahigh pressure metamorphic rocks from the Dabie–Sulu orogen in China: implications for geodynamics and fluid regime. Earth-Science Reviews 62, 105–161.
Zheng, Y.F., Wu, Y.B., Chen, F.K., Gong, B., Li, L., Zhao, Z.F., 2004. Zircon U–Pb and oxygen isotope evidence for a large-scale ^{18}O depletion event in igneous rocks during the Neoproterozoic. Geochimica et Cosmochimica Acta 68, 4145–4165.